Long-term P weathering and recent N deposition control contemporary plant-soil C, N and P

J.A.C. Davies[a], E. Tipping[b], E.C. Rowe[c], J.F. Boyle[d], E. Graf Pannatier[e], & V. Martinsen[f]

[a] Lancaster Environment Centre, Lancaster University, LA1 4YQ, UK

[b] Centre for Ecology and Hydrology, Library Avenue, Lancaster LA1 4AP, UK

[c] Centre for Ecology and Hydrology, Bangor, UK.

[d] University of Liverpool, UK.

[e] Swiss Federal Institute for Forest, Snow and Landscape Research WSL, Birmensdorf, Switzerland.

[f] Norges Miljø- Og Biovitenskaplige Universitet (NMB) Aas Norway

Key Points

- A new C N P model is compared with data from 88 natural sites in N. Europe.
- Weatherable P is an important long-term control on contemporary soil C and N.
- The model predicts large effects of N deposition on ecosystem C and N.

Abstract

Models are needed to understand how plant-soil nutrient stores and fluxes have responded to the last two centuries of widespread anthropogenic nutrient pollution and predict future change. These models need to integrate across carbon, nitrogen and phosphorus (C, N, & P) cycles and simulate changes over suitable timescales using available driving data. It is also vital that they are constrainable against observed data to provide confidence in their outputs. To date, no models address all of these requirements. To meet this need, a new model, N14CP, is introduced, which is initially applied to Northern hemisphere temperate and boreal ecosystems over the Holocene. N14CP is parameterized and tested using 88 northern Europe plot-scale studies, providing the most robust test of such a model to date. The model simulates long-term P weathering, based on the assumption of a starting pool of weatherable P (P_{weath0}, g m^{-2}), which is gradually transformed into organic and sorbed pools. Nitrogen fixation (and consequently primary production) is made dependent on available P. In the absence of knowledge about the spatial variability of P_{weath0}, N14CP produces good average

soil and plant variables, but cannot simulate variations among sites. Allowing P_{weath0} to vary between sites improves soil C, N and P results greatly, suggesting contemporary soil C, N and P are sensitive to long-term P weathering. Most sites were found to be N limited. Anthropogenic N deposition since 1800 was calculated to have increased plant biomass substantially, in agreement with observations, and consequently increased soil carbon pools.

1. Introduction

Over the last 200 years, the flows of carbon (C), nitrogen (N), and phosphorus (P), and many trace elements, have been modified by increasing population density, intensification of agriculture and emissions from fossil fuel burning. These disturbances are set to continue, and become even more widespread with the need to meet global food and energy needs. Understanding changing nutrient cycles in natural environments is important for understanding and managing future C stocks, water quality and biodiversity. In this study, a new model of C, N & P cycles, N14CP is described, tested and used to explore long-term and large-scale implications of anthropogenic atmospheric N pollution [*Galloway et al.*, 2004; *Sutton et al.*, 2013] in non-agricultural ecosystems.

Whilst the disturbed C cycle has been the main focus of scientific and public attention, the presence of biological actors within the earth system, with their requirements for C, N and P means that the cycling of these elements are tightly coupled. As such, it is problematic to consider one element in isolation. Terrestrial ecosystems that were once effectively closed with respect to nitrogen and phosphorus have become exporters of these nutrients, leading to eutrophication, acidification, loss of biodiversity and emission of greenhouse gas N_2O [*B Emmett et al.*, 2010; *Galloway et al.*, 2004; *van Vuuren et al.*, 2010; *Vitousek et al.*, 1997].

To understand and manage ecosystem changes at large spatial and temporal scales, quantitative models are needed for exploring and predicting the changes in soil stores of C, N and P, fluxes of these nutrients to air and water, and ecosystem response. These models must integrate cycles of C, N and P, and be capable of simulating large areas over long periods that reflect current understanding of process timescales e.g. C residence time in soil is in the centuries/millennia range for the bulk of soil organic matter (SOM) [*R Mills et al.*, 2014].

Many models incorporate C and N cycles – at least 250 as analyzed by *Manzoni and Porporato* [2009]. Far fewer models include P cycling. The CENTURY model [*Parton*, 1996] and CLM-CNP model [*X Yang et al.*, 2014] are exceptions which integrate C, N, and P

cycles. However, applications of CENTURY have largely concentrated on C and N, and where P outputs have been compared to data, these have been at the single-site scale [*Parton et al.*, 2005; *Raich et al.*, 2000]. Likewise, the CLM-CNP model, which concentrates on tropical ecosystems, compares results with observations of net primary productivity but not nutrient pools and fluxes. The TOTEM model also encompasses C, N, and P cycles, but in contrast to CENTURY and CLM-CNP, TOTEM simulates at a lumped global scale [*Mackenzie et al.*, 2002; *Ver et al.*, 1999]. The focus within TOTEM is the global C cycle, and as such testing against N and P data is not explored. More recently, attempts at distributed modeling at the global scale have been made. *Wang et al.* [2010] developed a global representation of C, N and P cycles to explore the spatial extent of N and P limitation and *Goll et al.* [2012] have incorporated P cycling into JSBACH. However, calibration and testing against P measurements have been limited in both of these cases. *Wang et al.* [2010] stated that a rigorous calibration of their model was not undertaken due to lack of global scale data, and used only leaf N:P ratio data, global soil %N estimates, and estimates of soil P fractions. Although their model was evaluated against measurements or estimates of biomass, soil C pool and litter production (which are indirectly controlled by P), evaluation directly relating to P was only carried out against P leaching data. *Goll et al.* [2012] used several P cycling parameters from *Wang et al.* [2010] in their extended version of JSBACH and calibrated biochemical mineralization fluxes from estimates of global soil N:P ratios.

If we are to have confidence in the use of large-scale models to address the wider ecosystem effects of disturbed C, N and P cycles, it is important to constrain and test them using field observations. A new model, N14CP, is proposed, which is simple enough in terms of its level of detail and input requirements to be applied over long timescales and at spatial scales beyond the site scale, but also suitable for testing using site-based data. This model builds upon an existing model of C, and N cycles, N14C [*E Tipping et al.*, 2012]. The aim is to create a C-N-P model suitable for a broad range of sites, that can be driven with readily available climate, deposition and soil data, to allow regional application that is informed by and tested against observed C, N and P data, rather than a site-specific model that cannot be generalized, or a large-scale model that is unconstrained against data.

Here, outcomes from the parameterization and testing of N14CP are reported, using soil C, N, P, radiocarbon, DOC, DON, and N leaching data for 88 post-glacial northern European sites including broadleaf and coniferous forests, shrublands and grasslands, young ecosystems with comparatively high soil P availability. The parameterized model is then used to explore

the role of P in determining ecosystem C and N stores and fluxes, and ecosystem responses to elevated atmospheric N deposition occurring over the last two centuries.

2. Methods

2.1. N14CP - A long-term regional scale C-N-P model

The N14C model [*E Tipping et al.*, 2012] of C and N cycles was developed to explore the influence of atmospheric N deposition on terrestrial semi-natural ecosystems. It provided a general parameterization (made against a set of plot-scale data), which could operate across multiple sites, and be driven with readily accessible data such as mean annual temperature, mean annual precipitation and N deposition. N14C also simulated radiocarbon (^{14}C) dynamics to constrain the turnover rates of the soil organic matter compartments within the model. The current study extends the N14C model with a simple treatment of P cycling, base cation (BC) weathering and pH to produce the N14CP model.

In the following subsections, a summary of the functionality of N14C is given, and then the extensions that form N14CP are described. Variables and parameters are listed in Tables 1 and 2, and a full model description is provided in the supporting information (SI).

2.1.1. Summary of the N14C model

The model simulates a number of linked C and N pools representing vegetation biomass, and soil organic matter (SOM) in two layers – a topsoil layer representing the first 15cm (to make these values comparable with survey data) and a subsoil layer representing everything below this depth. The model runs on a seasonal (3-month) timestep. The structure of N14C is depicted in the schematic in Figure 1.

In both N14C and N14CP, four plant functional types (PFTs) are represented: broadleaf, coniferous, herbaceous vegetation and shrubs. These represent the dominant PFT at a given site. The vegetation biomass comprises coarse woody and fine soft tissue, defined in terms of C:N ratio for each PFT. The C:N ratio of coarse tissue is constant, but that of fine tissue varies depending upon available N, thereby representing either a transition from N-poor to N-rich species or an enrichment of the fine tissues within a single species, or the combined effect of both. The variation in fine tissue C:N is implemented using a mix of two end

members with a high and a low C:N. Following Liebig's Law of the Minimum, net primary productivity (NPP) in N14C depends on a single limiting factor, which may be temperature, precipitation or available N.

Nitrogen enters the system from two sources: N deposition and N fixation. The N14C model assumes that N fixation is a fixed value based on literature values, which is down-regulated by atmospheric additions of N. This down-regulation remains a feature within the N14CP, but the fixation is now related to the availability of P, as described in Section 2.1.4.

At each quarterly time step, a fraction of the biomass C is converted to litter. Some of the associated N is also converted, while some is retained by the plant for reuse. The coarse litter does not enter the soil organic matter (SOM) pool, but decomposes at the soil surface, contributing N to the soil, but not C. The fine litter contributes to SOM, which is sectioned into three pools, each undergoing first-order decomposition reactions with turnover rates ranging from c. 2 to c. 1000 years following the formulation of *van Veen and Paul* [1981], which is shared by other models such as CENTURY [*Parton*, 1996]. These decomposition rates are modified by a temperature term, where the turnover rates are increased by a factor of Q_{10} for every 10°C increase in temperature

The C loss from decomposition is partitioned into CO_2 and DOC. Nitrogen is lost in proportion to C, consistent with the C:N stoichiometry of each SOM pool, and the N released is partitioned into inorganic N and DON in proportion to the partitioning of released C. The remaining decomposed N is inorganic and, in addition to the inorganic N from deposition, undergoes denitrification according to a temperature dependent first-order reaction. The residual inorganic N, together with the N retained within the plant prior to litterfall forms the available N for plant growth. If inorganic N remains after plant uptake, immobilization into SOM occurs, and any excess inorganic N is leached.

The SOM in the subsoil layer is fed by organic leachates from the topsoil layer in line with the ideas of [*Kaiser and Kalbitz*, 2012]. The SOM is represented in the subsoil by a single pool with one turnover rate.

2.1.2. N14CP weathering inputs of phosphorus and base cations

In N14CP, P and BCs can enter the plant-soil system by both weathering, i.e. dissolution of parent minerals, and, in principle, atmospheric deposition. Starting pools of weatherable P and BC (P_{weath} and BC_{weath}) are assumed, from which annual releases, ΔP_{weath} and

ΔBC_{weath}, are determined by first-order rate constants k_{Pweath} and $k_{BCweath}$ respectively. It is assumed that if the temperature is below zero, then no weathering occurs. This temperature dependency is implemented on an annual basis (like N14C, the majority of the model runs on a seasonal timestep, with weathering and pH estimation being exceptions to this) by multiplying the rate constant by the fraction of the year with a mean quarterly temperature above zero (according to climate input data), $F_{T>0}$. More formally:

$$\Delta P_{weath} = \mathrm{F_{T>0}} k_{\mathrm{Pweath}} P_{weath} \quad (1)$$

$$\Delta BC_{weath} = \mathrm{F_{T>0}} k_{\mathrm{BCweath}} BC_{weath} \quad (2)$$

where ΔP_{weath} and ΔBC_{weath} are assumed to enter the topsoil layer of the model and ΔP_{weath} is spread evenly over the quarterly time steps and contributes to an available pool of soil water P, P_{avail}.

The process of weathering here is highly simplified, due to the uncertainties surrounding other factors. Temperature and moisture are known to directly control weathering through their influence on chemical kinetics. The influence of temperature is only crudely incorporated within the model at present since although there is much evidence for temperature effects in laboratory experiments [e.g. *Brady and Carroll*, 1994; *White et al.*, 1999] , the influence of temperature in the field is harder to observe and difficult to decouple from other climate-related effects. Inhibition of weathering product release due to saturation of soil water, or conversely the reduction of rate limitation due to removal of weathering products by water flow have also been neglected here since the influence of water flow pathways on the contact time between water and rock is highly complex and uncertain. The influence of soil shielding on weathering [*Hartmann et al.*, 2014], i.e. the disconnection of the topsoil from the source material by soil thickness development, is not explicitly included as this is not a primary issue for the relatively young post-glacial soils of northern Europe. However, the first-order approximation of declining P_{weath} and BC_{weath} stock to some degree simulates a disconnecting effect over time. Vegetation and mycorrhizal fungi are recognized to have an influence on weathering processes, through the action of root exudates and nutrient seeking hyphae [*Berner*, 1992; *Knoll and James*, 1987; *Moulton and Berner*, 1998; *Moulton et al.*, 2000; *Pennington*, 1984; *Quirk et al.*, 2012; *L Taylor et al.*, 2009; *L L Taylor et al.*, 2012; *Volk*, 1987]. However, biota enhanced weathering was omitted here, as the extent to which weathering is controlled by biological activity and the manner in which this should be represented is still under debate.

Whereas P from weathering is intrinsic to the N14CP modelling (see Section2.1.3.), the weathering of BCs is only included to allow estimation of the soil water pH, which acts as a control on various soil processes (Section 2.1.3.). Neither the long-term accumulation of BCs by adsorption to soil solids nor their uptake into plants is simulated.

2.1.3. Soil pH in N14CP

Soil pH is added to the N14CP model, and is calculated annually from (a) the atmospheric depositional inputs of sulphate and BCs, (b) weathering inputs of BCs (eqn. 2), (c) simulated fluxes of inorganic N (assumed to be nitrate) and DOM, and (d) soil pCO2 (see Section S1.5). The pH-dependence of soil processes is quantified by a factor α_{pH} given by:

$$\alpha_{pH} = \left(1 + \left(\frac{[H^+]}{K_{acid}}\right)^{n_{acid}}\right)^{-1} \quad (3)$$

The values of K_{acid} and n_{acid} are defined such that this function allows for a variety of curves where α_{pH} varies between 0 and 1, increasing with pH. This approach is used to modify the decomposition of organic matter and the immobilization of N and P by OM (eqns. 10 and 12).

2.1.4. Phosphorus pools

Phosphorus pools are added to the N14C model to form N14CP as illustrated in Figure 1. Biomass P pools are linked to those of C and N, and C:N:P stoichiometries are defined for each PFT. A decomposing coarse litter P pool and soil organic phosphorus (SOP) pool are simulated alongside C and N and are subject to the same turnover rate constants i.e. the rate constants apply to SOM rather than C, N and P separately. There is no explicit speciation of organic P, although the three SOM fractions implicitly represent organic P fractions with differing turnovers. The factor α_{pH} is used to modify the decomposition rate

A topsoil pool P_{sorb} represents inorganic phosphorus sorbed to soil mineral surfaces, encompassing both occluded and non-occluded P. Sorption and desorption of inorganic P from P_{sorb} are determined by the parameters k_{sorb} and k_{desorb}, first-order rate constants that relate P_{sorb} to the dissolved excess inorganic P following growth P_{excess} i.e.:

$$\Delta P_{sorb} = k_{sorb} P_{excess} \quad (4)$$

$$\Delta P_{desorb} = k_{desorb} P_{sorb} \quad (5)$$

We did not attempt to modify P sorption, because its complex pH dependence (mid-range pH minimum; [*Weng et al.*, 2011]) precluded extraction of meaningful parameters from field data. A second sorbed P pool, subject to the same dynamics, is simulated in the subsoil layer alongside P in a subsoil SOP pool with one turnover rate.

2.1.5. N14CP plant growth

P is included as a limiting factor to plant growth alongside N, temperature and precipitation within a law-of-the-minimum approach. The potential net primary production (NPP_{pot}) in the model is determined, as in N14C. The actual net primary productivity (NPP_{act}) is then calculated by taking nutrient limitation into account i.e. the NPP is calculated based on N availability and P availability separately, and then the lower equates to NPP_{act}. P availability for plant growth is defined:

$$P_{avail} = \Delta P_{retained} + \Delta P_{decomp} + \Delta P_{rot} + \Delta P_{desorb} + \Delta P_{weath} + \Delta P_{DO} + P_{cleave} \quad (6)$$

Where $\Delta P_{retained}$ is the P that was remobilized and retained within the plant before the previous litterfall, ΔP_{decomp} and ΔP_{rot} are the inorganic P released from decomposition of the SOM and coarse litter pool respectively, ΔP_{DO} is the dissolved organic P, and P_{cleave} are the organic forms of P that may be accessible to plants through cleaving of bonds by extracellular phosphatase enzymes [*McGill and Cole*, 1981; *Olander and Vitousek*, 2000; *Rowe et al.*, 2008]. To ensure that including this source does not deplete the SOM reservoir unrealistically (i.e. beyond the range of soil N:P observations), the P which may be cleaved from the SOM is assumed to be limited by a maximum C to P ratio, $[C:P]_{fixlim}$ as follows:

$$P_{cleave} = P_{SOM} - \frac{C_{SOM}}{[C:P]_{fixlim}} \quad (7)$$

The sources of P to plant growth in eqn. 5 are used preferentially in their order of listing i.e. P retained within the plant is used first, then readily available inorganic P in soil water is used ($\Delta P_{decomp} + \Delta P_{rot} + \Delta P_{desorb} + \Delta P_{weath}$), followed by less accessible organic forms ΔP_{DO} and P_{cleave} from the SOM only where the P requirement indicated by the potential NPP exceeds the retained and inorganic sources.

2.1.6. Phosphorus-dependent nitrogen fixation

It is widely assumed that N fixation is to some extent controlled by P availability [*Cleveland et al.*, 1999; *Crews et al.*, 2000; *Eisele et al.*, 1989; *Vitousek et al.*, 2010], and to reflect this a

simple functional relationship between N fixation and P availability is included in N14CP. Attempting to explicitly represent the specific availability of P to particular N fixing organisms over time and space would be overly detailed in comparison to other process representation in the model. As such, a simple relationship between the overall amount of P in plant/microbe available forms and N fixation is made, minimizing the additional number of parameters needed. The overall amount of P in plant/microbe available forms $P_{fixavail}$ is defined equal to P_{avail} (eqn. 5), minus the plant retained P, which is used only for plant growth. N fixation is then assumed to take the following form:

$$\Delta N_{fix} = N_{fixmax} \frac{k_{Nfix} P_{fixavail}}{k_{Nfix} P_{fixavail} + 1} - \Delta N_{dep}(1 - f_{dep,bypass}) \quad (8)$$

Where N_{fixmax} is a temperature-dependent value determining the maximum fixation, k_{Nfix} is a constant controlling the degree to which P availability limits fixation, $f_{dep,bypass}$ controls the fraction of deposition that makes sustained contact with the topsoil.

Adding this dependency of N fixation on P availability means that, whilst a Law-of-the-Minimum approach is taken to calculating NPP, co-limitation can develop in the modelled system as advocated by *Danger et al.* [2008], through P limitation of N fixation.

2.1.7. Immobilization processes

In the N14C model [*E Tipping et al.*, 2012], if there was an excess of N after growth (ΔN_{excess}), then this would be available for immobilization into the SOM such that:

$$\Delta N_{immob} = k_{immobN} \Delta N_{excess} C_{SOM} Q_{10}^{T/10} \quad (9)$$

where k_{immobN} is the immobilization factor. This has been extended here to include a pH effect and stoichiometric effect such that:

$$\Delta N_{immob} = k_{immobN} \Delta N_{excess} C_{SOM} Q_{10}^{T/10} \alpha_{pH} \alpha_{C:N} \quad (10)$$

Where α_{pH} is a scalar that varies with pH as defined in equation 12, and $\alpha_{C:N}$ is a scalar that varies with current SOM C:N such that $\alpha_{C:N}$ is 0 below a C:N threshold $[\mathrm{C{:}\,N}]_{\mathrm{im,lower}}$, 1 above a C:N threshold $[\mathrm{C{:}\,N}]_{\mathrm{im,upper}}$ and a linear approximation between these thresholds:

$$\alpha_{C:N} = \left(\frac{\frac{C_{SOM}}{N_{SOM}} - [\mathrm{C{:}N}]_{\mathrm{im,lower}}}{[\mathrm{C{:}N}]_{\mathrm{im,upper}} - [\mathrm{C{:}N}]_{\mathrm{im,lower}}} \right) \quad (11)$$

where:

$$[\mathrm{C{:}\,N}]_{\mathrm{im,lower}} < \frac{C_{SOM}}{N_{SOM}} < [\mathrm{C{:}\,N}]_{\mathrm{im,upper}}$$

A proportionality constant $\beta_{immobP:N}$ is combined with the N immobilization constant so that P immobilization is defined:

$$\Delta P_{immob} = \beta_{immobP:N} k_{immobN} \Delta P_{excess} C_{SOM} Q_{10}^{T/10} \alpha_{pH} \alpha_{C:P} \quad (12)$$

Where $\alpha_{C:P}$ takes the same form as $\alpha_{C:N}$ (equation 11), but using C:P thresholds. Using a multiplier in this way relates the P immobilization rate constant to the N immobilization rate constant for each PFT using only one parameter.

2.1.8. Phosphorus losses

Phosphorus is lost from the topsoil by the leaching of any P_{inorg} that remains after plant uptake, immobilization and sorption. A fraction of this excess P_{inorg} enters the subsoil (Figure 1), where further sorption and desorption processes take place as in equation 4. Desorbed subsoil P_{inorg} is subsequently leached. Phosphorus is also lost from the topsoil in DOP, proportioned to DOC by the C:P stoichiometry of the SOM pools. As with DOC, some of the DOP accumulates in the subsoil.

2.2. Data for model parameterization and testing

Field site data comprising soil organic C, N and P pools, pH, and dissolved organic and inorganic element fluxes were compiled to calibrate and test the N14CP model (Tables S3-5). Measurements from broadleaf, coniferous, shrub and herbaceous semi-natural habitats were collated for 88 sites within northern Europe (Figure 2). Care was taken to create a dataset with equal numbers of the four PFTs, and encompassing a range of temperatures and soil pH. All sites have soil organic C and N measurements and soil pH, whilst 34 of the sites also have soil organic P data. The dataset was then split into two sets of 44 sites: one for model calibration, and one for model testing. Again, care was taken to ensure that the two sets had balanced numbers of PFTs, and were representative of the range of climate and soil conditions. All the data pertain to the topsoil (0-15cm), so topsoils are focused on in the model analysis and results.

All sites were simulated from 10000 BC, which is roughly the end of the last glaciation for northern Europe. It is assumed that at this time there was neither soil nor plant cover. Site conditions, including contemporary MAT, MAP, N, sulfur (S) and BC deposition were

compiled for each site. Site MAT was temporally varied using an anomaly based on [*Davis et al.*, 2003]. MAP was kept constant over the whole time period due to a lack of information on historical trends. Atmospheric deposition of N and S before 1800 was assumed to be zero i.e. pristine conditions without anthropogenic inputs were assumed. Whilst there were external inputs of N from lightning during this period, we estimate the magnitude of these to be in the region of 0.003-0.015 g m^{-2} a^{-1} based on [*Shepon et al.*, 2007] and [*Schumann and Huntrieser*, 2007]. These are small compared with rates of N fixation and so is neglected. Other natural sources of N, such as fires and soil NOx were ignored as these were not net exogenous inputs of N. Post 1800, the N, and S deposition (ΔN_{dep} and ΔS_{dep}) were assumed to follow the temporal anomaly suggested by [*Schöpp et al.* [2003]] and BC deposition (ΔBC_{dep}) followed a trend based on [*Majer et al.*, 0001]. These temporal trends were scaled to match contemporary observations available for each site modelled (Table S4 in the SI). Scavenging due to tree cover in included in the local measurements. Atmospheric P deposition was neglected as *Tipping et al.* [2014] have shown that there is no systematic variation of P deposition across Europe, and local re-distribution of P determines local gains and losses [*Tipping et al.*, 2014]. There is a net input of P to northern Europe from dust sources such as the Sahara [*Mahowald et al.*, 2008]. However, this input is small in comparison to weathering inputs, and given the uncertainty that surrounds further assumptions which would need to be made regarding historical changes in dust sources over the Holocene this source was assumed to be negligible.

A number of land use histories were defined for different geographical locations and land use types based on the characteristic timings of succession from herbaceous to wooded plant types following de-glaciation (that is if succession occurred at all) and woodland clearance dates. These are detailed within the SI, Table S5.

Representative radiocarbon contents of topsoils were assigned on the basis of vegetation cover: forested sites have been shown to have significantly higher radiocarbon values i.e. greater contents of recently-fixed C, than those of non-forested soils [*Bol et al.*, 1999; *R T E Mills et al.*, 2014; *Tipping et al.*, 2010; *E. Tipping et al.*, 2012]. Following *R T E Mills et al.* [2014], we assumed mean $SO^{14}C$ of 111.7 and107.9% modern for forest soils in 1971 and 2004 respectively. For non-forested soils, a mean $SO^{14}C$ of 99.1% modern for 2006 was assumed and for all sites a $DO^{14}C$ value of 109% modern for 2006 was adopted.

In the absence of measured values, a representative DOC:DOP ratio of 870 g g^{-1} was adopted, based on literature values [*Kaiser et al.*, 2003; *Lottig et al.*, 2012; *McGroddy et al.*, 2008; *Qualls and Haines*, 1991; *Yanai*, 1992]. The contemporary inorganic P leaching (ΔP_{inorg}) "target" for parameterisation was taken to be zero, but this does not mean that inorganic P leaching is prevented, rather that the present-day flux is constrained to be small.

PFT properties including: the ratio of coarse to fine plant tissues; the stoichiometric C, N and P contents of these tissues; and parameters determining litterfall characteristics; were set, as shown in Table S6 based on the sources detailed in the SI.

2.3. Model parameter sensitivity

Where possible, parameters were set based on literature values and parameters for processes shared by N14C and N14CP were assigned in keeping with *E Tipping et al.* [2012] (Table S2). The weathering rates k_{Pweath} and $k_{BCweath}$ were set in accordance with *Boyle et al.* [2013] to 2.5×10^{-4} and 6.3×10^{-5} respectively based on an analysis of lake sediment records and soil chronosequences. The initial base cation pool, BC_{weath0}, was estimated from contemporary pH measurements. The present day flux of BCs needed to provide the correct pH was calculated, utilizing site or mean levels of DOC and inorganic N leaching, and the site based N and S deposition. This flux was then used to determine the weathering pool needed at this date. A back calculation was then made to project this pool back to the initial condition, based on the known historical temperature.

There remain 10 parameters associated with the new process representations to be defined: $\beta_{immobP:N}$, f_{DO}, K_{acid}, N_{acid}, k_{Psorb}, $k_{Pdesorb}$, k_{Nfix}, $[C:P]_{lower}$, $[C:P]_{high-low}$, and $[P:C]_{lim}$. In addition, a parameter was required to characterize the variation of P_{weath0}. As will be explained in Section 3, after exploring the use of a constant value for P_{weath0}, and attempting to relate P_{weath0} to lithological and soil data for the different sites, the best approach we could find for parameterizing the present data set was to distinguish two sets of soils, podzols and rankers on the one hand, and all remaining soil types on the other. The adjustable parameter then was P_{weath0} for podzols and rankers, with a constant multiplier used to obtain P_{weath0} for the other soils.

We performed a sensitivity analysis to establish which of the 11 parameters have the most influence on the outputs of the model that can be compared against the observations, thus indicating which parameters are most worth exploring and which are insensitive and can be

set. The elementary effects method [*Campolongo et al.*, 2007], which considers parameter interactions, was used within the sensitivity analysis. The methodology, applications and results are described further in the SI (Section S2). Overall, the most influential parameters on the outputs are, in order of sensitivity: the fraction of adsorption of P onto mineral surfaces (k_{Psorb}); the factor which controls the fraction of C, N and P from decomposition which is lost in a dissolved organic form (f_{DO}); the initial pool of weatherable P (P_{weath0}); and the parameter relating N fixation to available P (k_{Nfix}). The least influential parameters are $[C:P]_{lower}$, $[C:P]_{high-low}$ and $[P:C]_{lim}$.

As a result of this analysis k_{Psorb}, f_{DO}, P_{weath0}, k_{Nfix}, $\beta_{immobP:N}$, K_{acid}, and N_{acid} were explored within the parameterization and $[C:P]_{lower}$, $[C:P]_{high-low}$ and $[P:C]_{lim}$ were fixed *a priori*. Although $k_{Pdesorb}$ was shown to have little influence on the majority of observable outputs, it was also explored within the parameterization as it is the most sensitive parameter in determining the inorganic P leaching flux and it is coupled closely to k_{Psorb}.

2.4. Model parameterization and testing

Half of the sites contained within the dataset described in Section 2.2 were used for parameterization, leaving half for blind testing. For the parameterization sites a cost function to assess the performance of the parameter set was constructed using observations of SOC, SON, SOP pools, soil C:N and N:P, DOC, DON and inorganic N leaching. In addition, non-site-specific values of NPP, $SO^{14}C$, $DO^{14}C$, DOC:DOP and ΔP_{inorg} (as described in 2.2.) were also used within this function. Multiple local searches were used to set well-constrained parameters, and a global search used to set less well-constrained parameters. Further details of the methodology are given in SI, Section S2.2. The general parameter set obtained by this procedure was subsequently tested against data from the remaining 44 sites.

A second parameterization exercise was undertaken where P_{weath0} was varied on a site by site basis for all the sites within the dataset, whilst all other parameters were kept at their generalized values. For each site, P_{weath0} was systematically varied between 50 and 1000 g m^{-2}, since these values gave initial and contemporary P weathering rates in the range 0.75 to 150 kg km^{-2} a^{-1}, covering the range of values (1.5 to 85 kg km^{-2} a^{-1}) estimated by [*Hartmann et al.*, 2014]. The site-specific observations of SOC, SON, SOP pools, soil C:N, DOC, DON and inorganic N leaching were then used within a cost function to calibrate P_{weath0} for each site (S2.3 details this further).

3. Results

3.1 N14CP Model parameterization and testing

Preliminary trials with N14CP showed that the simulated contemporary soil organic P pool (P_{SOM}), depended strongly upon the value of P_{weath0}, as must be expected for soils of similar age assumed to have undergone the same development processes with respect to the different P pools. Therefore, we sought a predictor of P_{weath0} correlated to the measured P_{SOM}, which ranged from 10 to 80 g m^{-2}. We explored the use of globally-mapped lithological data *[Hartmann and Moosdorf, 2011; 2012; Hartmann et al., 2012; Hartmann et al., 2014; Xiaojuan Yang et al., 2013]*, but no correlation with P_{SOM} was found using either rock P concentration or P weathering rate (r^2 = 0.0, n = 47 in both cases). Secondly, we considered soil types, and found that the average P_{SOM} for the podzols and rankers with measured P_{SOM} (n = 21) was significantly lower ($p < 0.02$), by a factor of 1.7, than the average for other soil types (n = 26). We used this finding in the general modelling to distinguish P_{weath0} among sites, parameterizing the value for podzols.

The general parameter set is given in Table 3, and model results are plotted against observations for the 44 parameterization and 44 testing sites in Figure 3 (left and middle columns respectively). The general model reproduced mean observed variables satisfactorily for both the parameterization and test sites, however, all r^2 values in both cases were zero or close to zero (means, r^2 values and root means square errors are reported in Figure 3). There were positive correlations between observations and modeled values for soil C, N and P, the soil C:N ratio, and DON, although none were significant. There were no correlations between the observed and modelled DOC and dissolved inorganic N fluxes. For the test data set, correlations between observed and modelled soil C, N and P were weakened, but the correlations for inorganic N leaching and soil C:N ratio were strengthened, and were significant ($p<0.05$ and $p<0.005$ respectively). Root mean squared errors (RMSE) between observations and predictions did not systematically decrease between parameterization and test sites. Overall, there was not a consistent degradation in model performance between parameterization and testing.

The right-hand column of Figure 3 shows that model performance across soil nutrient pools was markedly improved by allowing P_{weath0} to vary on a site-by-site basis, as described in Section 2.4. Correlations between modelled and observed outputs were increased, and all

were significant ($p<0.001$). The intercepts of these correlations were also reduced bringing the results closer to the one-to-one line. Positive r^2 values were produced for the C, N and P soil pools by the P_{weath0} site calibrated results, and RMSE values were reduced.

The resultant site-specific P_{weath0} values were log-normally distributed between 50 and 720 g m^{-2} with a geometric mean of 145 g m^{-2} (Figure S5). As expected, a strong ($r^2 = 0.60$, $p < 0.001$) positive correlation is found between site-specific P_{weath0} and measured P_{SOM}. The mean site-specific P_{weath0} value for podzols and rankers is lower than the mean for other soils, by a factor of 1.2, in line with the observed difference in topsoil P_{SOM} between these soil groups. However the difference was not significant ($p>0.25$). No relationship of site-specific P_{weath0} with pH ($r^2 = 0.03$, $p > 0.1$) was found, nor with PFT, nor geographical location (Figure S5).

3.2 Time series results

Using generalized parameter set, we examined general temporal trends in system C, N and P using four generic sites (one for each PFT), driven by median climate and deposition forcings. The soil type was set to podzolic for each of the four sites. Figures 4-6 give results for these generic sites.

The calculated initial accumulation rates of C, N and P are such that the C pool took approximately 4000 years to reach 1000 g m^{-2} (Figure 4), which is appreciably slower than found in most chronosequence or recolonization studies [*Anderson*, 1977; *Jones et al.*, 2008; *Mavris et al.*, 2010; *Phillips et al.*, 2008; *Richardson et al.*, 2004]. This may reflect underestimation of the N fixation rate under early conditions, because our modelling of N fixation, dependent only upon P availability and temperature (eqn. 11), is too simple, for example neglecting early colonization by N-fixers [*S K Schmidt et al.*, 2008]. However, contemporary early soil formation may be influenced by neighboring [*Anderson*, 1977], N deposition [*Jones et al.*, 2008] and higher temperatures and therefore not be directly comparable to conditions following deglaciation. Nonetheless, the C, N and P pools subsequently build up to reach realistic levels by 5000 BP (i.e. 3000 BC), after which they change only slowly, although true steady states are not attained.

Between 1800 and 2000, the increasing influence of anthropogenic atmospheric N deposition caused 1.9 to 3.3-fold increases in NPP attributable to elevated N deposition (Figure 4). Likewise topsoil C pools increase 1.25 to 2 times and topsoil N pools increase 1.2-1.8 times

over this period. Topsoil P declines, however, as elevated N deposition alleviates N limitation of NPP and increasing quantities of P are acquired from the SOM to support this growth. Also, larger pools of C and N in the soil lead to greater production of DOM, given the constant turnover rates. As such, there is also a contemporary rise in P loss via DOP.

Comparing the PFTs, the N14CP model shows marked differences in SON between tree and non-tree plant types, with lower soil N under trees. This is attributable to the larger biomass pools of N and P in the tree PFTs within the model. The difference between tree and non-tree PFTs is also borne out in the field data, with topsoil organic N pools being significantly higher in shrub and herbaceous sites than broadleaf and deciduous sites ($p < 0.001$), with means of 438 g-N m^{-2} and 316 g-N m^{-2} respectively. The modelled broadleaf site (Figure 4) shows the strongest response to the elevated N deposition as this site receives the most deposition (the PFT N deposition median is highest for broadleaf sites), and subsequently has the biggest increase in plant available N (Figure 4). The response in topsoil N:P in broadleaf ecosystems is particularly marked, as an amplifying effect is seen as topsoil is enriched by deposition and P in the SOM is reduced as plants start to acquire P from this source for growth to stoichiometrically match the increasing N.

Comparing the results in Figure 4 to those of the C-N model of N14C [*E Tipping et al.*, 2012], generally the effects of N deposition on NPP and soil pools are of similar magnitudes. The pre-modern N fixation rate assumed in N14C based on literature values falls within the upper end of the range of N fixation rates simulated in N14CP. A rate of 0.3 g m^{-2} was used in N14C, and the rate in N14CP is 0.17-0.21 g m^{-2} (Figure 4) and 0.27-0.35 g m^{-2} for podzol/rankers and non-podzol/rankers respectively, as determined by the parameterization.

3.2.1. Phosphorus dynamics

At the start of the simulation all the P is in weatherable rock (Figure 5), and this source diminishes owing to leaching losses of P_{inorg} and DOP over time, so that the present total P pool is about 50% of the initial one. The temporal changes in soil P pools are in line with the findings of *TW Walker and Syers* [1976] and *Buendía et al.* [2010]. Initially, weathered P is mainly transferred to the sorbed pool, then the organic pool develops along with the biomass and soil N pools. The vegetation then diverts P from sorbing to soil surfaces, and by modern times the majority of P is stored within the SOP, as is observed for young temperate soils. However, as N availability increases with modern day N deposition, more available P is taken up in growth increasing the total P held within the vegetation pools. As plants can access P in

SOP within the model if there is sufficient N, then there is a reduction in SOP. It is also evident in these plots that, over long timescales, the rate of loss in P is declining. Dissolved inorganic leaching fluxes of P peak and decline in line with the soil inorganic P pool (Figure 6). The DOP initially increases with SOP. However, between 4000 and 2000 BC the vegetation starts accessing the DOP for growth, creating a decline in the DOP leaching rate from 4000 BC to 1800 AD.

If a non-podzol/ranker soil is assumed then the initial pool of weatherable P is larger, resulting in larger topsoil organic C, N and P pools in the order of 10-20% for C, 20-50% for N and 65-140% for soil P. These larger pool sizes are attributable to long term changes in N fixation rather than increased P availability in the short term i.e. contemporary NPP is not significantly increased (0.1-3%). This indicates that the sensitivity of contemporary soil C, N and P pools to the P weathering source results from the links made between N fixation and P availability.

4. Discussion

4.1. Weatherable P as a control on soil C, N and P

Fundamental to the development of these ecosystems is the weathering input of P, which not only acts as a plant nutrient but also affects biomass and carbon accumulation through its influence on N fixation. The results from site-specific variation of P_{weath0} (Figure 3, right hand column) demonstrate its strong effects on predicted contemporary soil C, N and P pools. When P_{weath0} is allowed to vary within sensible ranges for rock P content and P weathering fluxes, the improvements in the prediction of soil C and N, as well as soil P, are striking. This dynamic ecosystem modelling has quantitatively produced behaviors that agree with the deductions made on the basis of soil C, N and P concentrations by Walker and colleagues [*T. Walker and Adams*, 1958; *TW Walker and Syers*, 1976] regarding the key influence of P on the biogeochemical cycles of C and N, and on soil fertility.

In making comparisons of our estimates of P_{weath0} and P weathering rates with lithologically-based data [*Hartmann and Moosdorf, 2011; 2012; Hartmann et al., 2012; Hartmann et al., 2014; Xiaojuan Yang et al., 2013*], it needs to be borne in mind that because our model involves the dissolution of a specified amount of apatite, the weatherable pools and fluxes

change over time, as in the conceptual model of *TW Walker and Syers* [1976]. Thus, our analysis produces an average contemporary P weathering rate of about 0.003 g m^{-2} a^{-1}, while the initial rate was about 10 times higher. A different approach to the estimation of P weathering inputs is from the approach of *Hartmann and Moosdorf* [2012] who estimated them by combining the hydrochemical flux of Si (assumed not to be significantly affected soil processes) with P/Si rock ratios. From the mapped GLiM lithology [*Hartmann and Moosdorf*, 2012] and P weathering data by rock type [*Hartmann et al.*, 2014], an average weathering input of P at our field sites of about 0.012 g m^{-2} a^{-1} is obtained. This is bracketed by our initial and contemporary fluxes, and so the independent approaches (modelling and hydrogeology) yield order-of-magnitude agreement.

However, the site-specific model-derived weathering rates do not correlate with the lithologically-based values ($r^2 = 0.0$, $p > 0.7$, $n = 84$), which precludes the use of the latter in our modelling. The lack of correlation is perhaps not surprising given that the lithological mapping, although high resolution in global terms, is coarse at the scales of our sites. The average GLiM polygon has an area of c. 400 km^2, providing considerable scope for lithological and P source heterogeneity. The higher resolution of soil mapping, and the tendency of soil type to reflect parent mineral properties, probably explain the modest predictive power obtained by putting the sites into two classes (podzols/rankers and other soils), but we note that the significant difference between the two classes does not apply for the site-specific P_{weath0} values. Neither did we find any significant variation of P_{weath0} with geographical location, PFT or pH. Thus, currently available data sets offer little possibility of predicting P weathering or P_{weath0}, and associated spatial variability in soil C and N pools and ecosystem productivity. Predictive modelling is therefore restricted to average conditions over many sites, as in the first two columns of Fig 4. Systematic research is required to characterize field sites on soils with selected parent materials varying in P content, and then combine the results with dynamic modelling using N14CP and other models.

4.2. Nutrient limitations to plant productivity

In the model, NPP at all 88 sites was nutrient limited, rather than temperature or precipitation limited. The sites were predominantly N limited. Only one site was P limited for results using the general P_{weath0} values, rising to 15 P limited sites when using the site-specific P_{weath0}. Of the P-limited sites for the latter, there was no dominance of vegetation type or geographical location, however, the soils were predominantly podzolic (11 out of 15).

Interestingly, the mean N deposition to the P limited sites was significantly higher than that to the non-P limited sites ($p < 0.05$) and the observed N pools were also found to be significantly lower ($p < 0.001$). This suggests that the site-specific calibration of P_{weath0} has attributed low P availability to sites where observation of soil N are low given the level of N deposition, thus limiting development of soil N. This may actually be the case, or it is possible that the N deposition estimate for these sites is too high or soil observation of N is uncharacteristically low. It is also possible that the model has not sufficiently captured the cause of difference between sites. Only three of the P-limited sites have soil organic P observations, so it is difficult to determine whether the model is falsely predicting low P in these cases. However, for the three observations that were available, one site has lower modeled topsoil organic P (by 60%) and the other two have higher modeled topsoil organic P (by 17% and 48%), indicating that the model is not consistently underestimating P to account for a lack of N.

In N14CP, plant uptake of inorganic N and P is prioritised over their immobilisation into SOM, and as a result, for the N-limited systems that make up the great majority of our field sites, all available inorganic N is used for plant growth during the growing season, and (net) immobilisation occurs only during the non-growing season. This allows plant stoichiometric requirements for nutrients to be met and sensible values of NPP to be achieved, while the SOM can sequester N in the long term. Plainly, nutrient immobilization by microbes must actually occur during the growing season, but the implication is that recycling results in no net immobilization. As explained by *Kaye and Hart* [1997] this situation can arise because "*even if plants/mycorrhizae are relatively unsuccessful competitors for N during individual competition events, they can accumulate N for growth by competing several times for the same N atom and then storing N in plant tissues*". Thus at the quarterly time-step employed in N14CP, the simplifying assumption that plants have priority for nutrients during the growing season can be justified, and we assume it applies to both N and P. Consequential simulation outcomes are (a) zero inorganic N leaching rates from topsoil during the growing season, and (b) the removal (partial to nearly complete) of atmospherically-deposited N by the ecosystem. These predictions are in broad agreement with observed surface water NO_3-N fluxes in UK upland areas receiving high atmospheric N deposition; the fluxes are low in summer but relatively high in winter, although lower than atmospheric inputs [*Neal et al.*, 2003; *E. Tipping et al.*, 2008].

Our approach to modelling ecosystem development relies on the strong empirical evidence that productivity of temperate natural and semi-natural ecosystems is limited by N and sometimes P [*Elser et al.*, 2007; *Vitousek et al.*, 2010]. In N14CP, if neither of these nutrients is limiting, NPP is determined by either temperature or precipitation. We neglect possible CO_2 fertilization, which may be significant given that the atmospheric CO_2 concentration has risen by c. 40% since 1800, and is projected to be more than twice the 1800 value by the end of the 21st century [*IPCC*, 2014]. Some free-air CO_2 enrichment (FACE) experiments show an increase in forest NPP in response to a step-change of 200 ppmv in atmospheric CO_2 concentration; for example at the N-limited Duke University site an enhancement in NPP of c. 30% is reported [*McCarthy et al.*, 2010]. According to *Drake et al.* [2011] this could arise by the stimulation of soil microbial activity under elevated CO_2 causing a faster turnover of SOM and acceleration of N cycling. Such an effect might be incorporated into N14CP, via an empirical relationship between CO_2 concentration and SOM turnover rate constants. However, Drake et al. [2011] also pointed out that observed ecosystem responses to experimentally elevated atmospheric CO_2 concentration vary widely, from no response to transient and sustained increases in NPP. Furthermore, an assessment of the outputs of 7 forest models (appreciably more detailed than N14CP with respect to plant physiology and soil biogeochemistry) concluded that there are significant uncertainties especially in the N cycle that hamper prediction of CO_2 effects [*A P Walker et al.*, 2015]. Therefore, it is premature to include a representation of CO_2 effects in N14CP. It can also be noted that modelled increases in NPP over 300 years as a result of a step change in CO_2 concentration from 380 to 550 ppmv are typically 20% [*A P Walker et al.*, 2015], which is modest in comparison to the 200 to 300% increases simulated in response to N deposition in northern Europe (Figure 4).

4.3. Atmospheric N deposition and P

Increased atmospheric N deposition was shown to have a large effect on NPP and soil C and N pools in the model (Figure 4), which is understandable given that the sites were most commonly N limited. The calculated increase in tree biomass C over the period 1800-2000 (Figure 4) corresponds to an increase of 60 gC per g atmospherically-deposited N, or 30 gC gN^{-1} if only above-ground biomass is considered. This is about 50% of the value of 61 gC gN^{-1} estimated by *Quinn Thomas et al.* [2010] from US forestry inventory data, but is in the middle of the range of 15-40 gC gN^{-1} estimated for European forests by *de Vries et al.*

611 [2009]. Therefore, our calculated effects are quantitatively realistic, at least in terms of tree
612 NPP and biomass.

613 The magnitudes of increases in NPP, soil C and N agree with previous results from N14C,
614 which did not incorporate P cycling [*E Tipping et al.*, 2012], suggesting that whilst P is
615 important in long-term soil C and N development, P has not suppressed the response to N
616 deposition at these sites. By integrating the cycles of C, N and P, we can also examine the
617 influence of C and N on P. The model indicates that increases in N and C caused by
618 atmospheric N deposition may accelerate P loss in ecosystems by DOP leaching. Increased
619 turnover of newly sequestered C under elevated N levels will lead to a running down of P
620 within the soil as P is not renewed from exogenous sources, assuming decomposition of C, N
621 and P is under stoichiometric control, as is the case in N14CP.

622 *4.4 No significant pH effect on decomposition and immobilization*

623 The modelling revealed only a small dependence of SOM turnover or nutrient immobilization
624 on pH. This is contrary to the prevailing opinion that the rates of these processes are
625 significantly lower under acid conditions [*Leifeld et al.*, 2013; *Walse et al.*, 1998]. Evidently,
626 although the present data covered a range of soil pH (Figure 2), factors other than pH had
627 more influence on the model parameterization. It may be that the model would find a pH
628 dependence if the spatial data employed here were supplemented with time series data, for
629 example the observations of *Oulehle et al.* [2011] that in the Czech Republic forest floor
630 organic matter declined as a result of acidification reversal over the period 1995-2009.

631 *4.5 Extension to other ecosystem types*

632 The N14CP model in its current version simulates macronutrient behavior in temperate
633 ecosystems with young soils, with a sufficiently simple process representation to permit
634 parameterization from field data. This is already useful in the analysis and potential
635 prediction of C, N and P cycling in systems such as those of northern Europe that are
636 experiencing high N deposition. To make the model more globally applicable, i.e. extending
637 the approach to a wider range of ecosystems, additional factors would need to be considered.
638 Given the importance of P availability in ecosystem development, then over geological
639 timescales (c. 10^6 years) a significant issue is the replenishment of weatherable P by tectonic
640 uplift, as emphasized in the global P modelling of *Buendía et al.* [2010], which would need to
641 be added to the model to simulate ecosystems on older soils. The wider variations water

642 availability at global scales would need to be factored in with respect to both weathering and
643 element losses by leaching, secondary mineral formation, and temperature effects on
644 weathering (cf. [*Goll et al.*, 2014]) might need to be included. Element losses by physical
645 erosion would be more important in some ecosystems. The simulation of agricultural systems
646 would need to account for biomass removal in cropping, and the effects of intensive grazing.
647 The simulation of peatlands would require a version of the model able to deal with the burial
648 of carbon in the anoxic catotelm, and recognizing the importance to such systems of P inputs
649 by atmospheric deposition and biological transfers (Tipping et al., 2010). Basic field data
650 comprising soil variables, including radiocarbon data, and NPP, for parameterization and
651 testing could be applied at the global scale in a similar way to that adopted here. In addition,
652 chronosequence data (e.g. [*Richardson et al.*, 2004]) could be used. Working at the larger
653 scale would likely produce more insights through the more effective use of lithological data
654 (Section 4.1) to predict weathering rates, not only of P but also base cations, and mineral N
655 present in sedimentary rocks [*Morford et al.*, 2011].

656 # 5. Conclusions

657 A new model, N14CP, integrating terrestrial carbon, nitrogen and phosphorus cycles that is
658 suitable for long-term application (~10,000 years) in temperate/boreal northern hemisphere
659 ecosystems at regional scales has been presented. The model addresses an important
660 requirement for models that are applicable at scales above the site-scale, but constrainable
661 against observation data. The model has been parameterized and tested using field
662 observations from 88 sites in northern Europe across broadleaf, conifer, shrub and herbaceous
663 habitats, making it the most robustly tested model of C, N and P cycles to date. With
664 available driving data (climate, vegetation history, N deposition), it has been demonstrated
665 that the model can represent broad contemporary trends in nutrient change across multiple
666 soil nutrient pools and fluxes. However, smaller inter-site variation was not well reproduced.

667 The study highlighted the importance of weatherable P as a control on the long-term
668 development of ecosystem C, N, and P. This mainly arises because of the assumed
669 dependence of N fixation, and consequent C fixation, on P availability. Model performance
670 across C, N and P variables was considerably improved when the initial weatherable P was
671 allowed to vary site-by-site within boundaries reasonable for the variation in lithology. This
672 yielded a range of 50 to 720 g m^{-2} of weatherable P, and resulted in appreciable increases in
673 goodness of fit. However, we could not find a predictive variable in soil type, lithology or pH

etc. for this variation. Finer-scale spatial characterization of weatherable P is needed to determine if inter-site variation can be explained by this variable. Alternatively, a study analyzing model performance at regional scales against observations across systematically chosen lithological types would help determine whether available lithological data is informative for this purpose at larger scales.

All sites were found to be nutrient limited in the simulations, and most commonly N limited. As such, the model predicted that elevated N deposition since 1800 has considerably increased soil C and N and net primary productivity, under median conditions doubling or tripling NPP, leading to higher plant biomass. The increase in biomass C per N deposition ratio of 30 for median conditions is in line with literature data. The effects of N dep have not been suppressed by a lack of P, at least for the relatively young soils (~12000 years) of the sites examined.

6. Acknowledgements

We thank M. Vieno (Centre for Ecology and Hydrology) and B. Rihm (METEOTEST, Switzerland) for the provision of deposition data, C.L. Bryant (NERC Radiocarbon Facility) for advice on radiocarbon, A.F. Harrison (Centre for Ecology and Hydrology) for the provision of soils data and R. Tipping for help with data collation. We are also grateful to the Editor (S.Trumbore) and three referees for their constructive comments. All data can be requested from the corresponding author (Jessica Davies, j.davies4@lancaster.ac.uk). This research was funded by the UK Natural Environment Research Council Macronutrient Cycles Programme (LTLS project, Grant numbers NE/J011533/1 NE/J011703/1 and NE/J011630/1) and the Scottish Government.

7. References

Anderson, D. W. (1977), Early stages of soil formation on glacial till mine spoils in a semi-arid climate, *Geoderma*, *19*(1), 11-19.

Andersson, P., D. Berggren, and I. Nilsson (2002), Indices for nitrogen status and nitrate leaching from Norway spruce (Picea abies (L.) Karst.) stands in Sweden, *Forest Ecology and Management*, *157*(1), 39-53.

Beier, C., B. A. Emmett, A. Tietema, I. K. Schmidt, J. Peñuelas, E. K. Láng, P. Duce, P. De Angelis, A. Gorissen, and M. Estiarte (2009), Carbon and nitrogen balances for six shrublands across Europe, *Global Biogeochemical Cycles*, *23*(4).

Berggren, D., B. Bergkvist, M.-B. Johansson, P.-A. Melkerud, A. Nilsson, M. Olsson, O. Langvall, H. Majdi, and P. Weslien (2004), A description of LUSTRA's common field sites*Rep.*, Swedish Univ. of Agricultural Sciences, Uppsala (Sweden). Dept. of Forest Soils.

Berner, R. A. (1992), Weathering, plants, and the long-term carbon cycle, *Geochimica et Cosmochimica Acta*, *56*(8), 3225-3231.

Blaser, P., S. Zimmermann, J. Luster, L. Walthert, and P. Lüscher (2005), Waldböden der Schweiz. Band 2. Region Alpen und Alpensüdseite. Birmensdorf, WSL, Bern, edited, Hep Verlag.

Bloemerts, M., and W. d. Vries (2009), Relationships between nitrous oxide emissions from natural ecosystems end environmental factors.

Bol, R. A., D. D. Harkness, Y. Huang, and D. M. Howard (1999), The influence of soil processes on carbon isotope distribution and turnover in the British uplands, *European Journal of Soil Science*, *50*(1), 41-51.

Boyle, J. F., R. C. Chiverrell, S. A. Norton, and A. J. Plater (2013), A leaky model of long-term soil phosphorus dynamics, *Global Biogeochemical Cycles*, *27*(2), 516-525.

Brady, P. V., and S. A. Carroll (1994), Direct effects of CO< sub> 2</sub> and temperature on silicate weathering: Possible implications for climate control, *Geochimica et Cosmochimica Acta*, *58*(7), 1853-1856.

Buendía, C., A. Kleidon, and A. Porporato (2010), The role of tectonic uplift, climate, and vegetation in the long-term terrestrial phosphorous cycle, *Biogeosciences*, *7*(6), 2025-2038.

Campolongo, F., J. Cariboni, and A. Saltelli (2007), An effective screening design for sensitivity analysis of large models, *Environmental Modelling & Software*, *22*(10), 1509-1518.

Cleveland, C. C., A. R. Townsend, D. S. Schimel, H. Fisher, R. W. Howarth, L. O. Hedin, S. S. Perakis, E. F. Latty, J. C. Von Fischer, and A. Elseroad (1999), Global patterns of terrestrial biological nitrogen (N2) fixation in natural ecosystems, *Global Biogeochemical Cycles*, *13*(2), 623-645.

Corre, M. D., and N. P. Lamersdorf (2004), Reversal of nitrogen saturation after long-term deposition reduction: impact on soil nitrogen cycling, *Ecology*, *85*(11), 3090-3104.

Crews, T. E., H. Farrington, and P. M. Vitousek (2000), Changes in asymbiotic, heterotrophic nitrogen fixation on leaf litter of Metrosideros polymorpha with long-term ecosystem development in Hawaii, *Ecosystems*, *3*(4), 386-395.

738 Danger, M., T. Daufresne, F. Lucas, S. Pissard, and G. Lacroix (2008), Does Liebig's law of
739 the minimum scale up from species to communities?, *Oikos*, *117*(11), 1741-1751.

740 Davis, B. A. S., S. Brewer, A. C. Stevenson, and J. Guiot (2003), The temperature of Europe
741 during the Holocene reconstructed from pollen data, *Quaternary Science Reviews*, *22*(15–17),
742 1701-1716.

743 de Vries, W., G. Schütze, S. Lofts, E. Tipping, M. Meili, P. Römkens, and J. Groenenberg
744 (2005), Calculation of critical loads for cadmium, lead and mercury; background document to
745 a mapping manual on critical loads of cadmium, lead and mercury*Rep.*, Alterra.

746 de Vries, W., S. Solberg, M. Dobbertin, H. Sterba, D. Laubhann, M. Van Oijen, C. Evans, P.
747 Gundersen, J. Kros, and G. Wamelink (2009), The impact of nitrogen deposition on carbon
748 sequestration by European forests and heathlands, *Forest Ecology and Management*, *258*(8),
749 1814-1823.

750 DEFRA UK Research on The Eutrophication and Acidification of Terrestrial Ecosystems
751 edited, http://ukreate.defra.gov.uk/index.htm.

752 defra UK Acid Waters Monitoring Network, edited.

753 Drake, J. E., A. Gallet-Budynek, K. S. Hofmockel, E. S. Bernhardt, S. A. Billings, R. B.
754 Jackson, K. S. Johnsen, J. Lichter, H. R. McCarthy, and M. L. McCormack (2011), Increases
755 in the flux of carbon belowground stimulate nitrogen uptake and sustain the long-term
756 enhancement of forest productivity under elevated CO2, *Ecology letters*, *14*(4), 349-357.

757 Eisele, l., D. Schimel, L. Kapustka, and W. Parton (1989), Effects of available P and N: P
758 ratios on non-symbiotic dinitrogen fixation in tallgrass prairie soils, *Oecologia*, *79*(4), 471-
759 474.

760 Elser, J. J., M. E. S. Bracken, E. E. Cleland, D. S. Gruner, W. S. Harpole, H. Hillebrand, J. T.
761 Ngai, E. W. Seabloom, J. B. Shurin, and J. E. Smith (2007), Global analysis of nitrogen and
762 phosphorus limitation of primary producers in freshwater, marine and terrestrial ecosystems,
763 *Ecology Letters*, *10*(12), 1135-1142.

764 Emmett, B., B. Reynolds, P. Chamberlain, E. Rowe, D. Spurgeon, S. Brittain, Z. Frogbrook,
765 S. Hughes, A. Lawlor, and J. Poskitt (2010), Countryside survey: Soils report from 2007.

766 Emmett, B. A., C. Beier, M. Estiarte, A. Tietema, H. L. Kristensen, D. Williams, J. Penuelas,
767 I. Schmidt, and A. Sowerby (2004), The response of soil processes to climate change: results
768 from manipulation studies of shrublands across an environmental gradient, *Ecosystems*, *7*(6),
769 625-637.

770 Evans, C., B. Reynolds, C. Curtis, H. Crook, D. Norris, and S. Brittain (2005), A conceptual
771 model of spatially heterogeneous nitrogen leaching from a Welsh moorland catchment,
772 *Water, Air, & Soil Pollution: Focus*, *4*(6), 97-105.

773 Galloway, J. N., F. J. Dentener, D. G. Capone, E. W. Boyer, R. W. Howarth, S. P. Seitzinger,
774 G. P. Asner, C. Cleveland, P. Green, and E. Holland (2004), Nitrogen cycles: past, present,
775 and future, *Biogeochemistry*, *70*(2), 153-226.

776 Goll, D., N. Moosdorf, J. Hartmann, and V. Brovkin (2014), Climate-driven changes in
777 chemical weathering and associated phosphorus release since 1850: Implications for the land
778 carbon balance, *Geophysical Research Letters*, *41*(10), 3553-3558.

779 Goll, D., V. Brovkin, B. Parida, C. Reick, J. Kattge, P. Reich, P. Van Bodegom, and Ü.
780 Niinemets (2012), Nutrient limitation reduces land carbon uptake in simulations with a model

781 of combined carbon, nitrogen and phosphorus cycling, *Biogeosciences Discussions*, *9*(3),
782 3173-3232.

783 Gundersen, P. (1995), Nitrogen deposition and leaching in European forests—preliminary
784 results from a data compilation, *Water, Air, and Soil Pollution*, *85*(3), 1179-1184.

785 Hartmann, J., and N. Moosdorf (2011), Chemical weathering rates of silicate-dominated
786 lithological classes and associated liberation rates of phosphorus on the Japanese
787 Archipelago—Implications for global scale analysis, *Chemical Geology*, *287*(3–4), 125-157.

788 Hartmann, J., and N. Moosdorf (2012), The new global lithological map database GLiM: A
789 representation of rock properties at the Earth surface, *Geochemistry, Geophysics,*
790 *Geosystems*, *13*(12), Q12004.

791 Hartmann, J., H. Dürr, N. Moosdorf, M. Meybeck, and S. Kempe (2012), The geochemical
792 composition of the terrestrial surface (without soils) and comparison with the upper
793 continental crust, *Int J Earth Sci (Geol Rundsch)*, *101*(1), 365-376.

794 Hartmann, J., N. Moosdorf, R. Lauerwald, M. Hinderer, and A. J. West (2014), Global
795 chemical weathering and associated P-release — The role of lithology, temperature and soil
796 properties, *Chemical Geology*, *363*(0), 145-163.

797 IPCC (2014), http://www.ipcc-data.org/observ/ddc_co2.html, edited.

798 Jackson-Blake, L., R. Helliwell, A. Britton, S. Gibbs, M. Coull, and L. Dawson (2012),
799 Controls on soil solution nitrogen along an altitudinal gradient in the Scottish uplands,
800 *Science of the Total Environment*, *431*, 100-108.

801 Jones, M. L. M., A. Sowerby, D. L. Williams, and R. E. Jones (2008), Factors controlling soil
802 development in sand dunes: evidence from a coastal dune soil chronosequence, *Plant Soil*,
803 *307*(1-2), 219-234.

804 Kaiser, K., and K. Kalbitz (2012), Cycling downwards – dissolved organic matter in soils,
805 *Soil Biology and Biochemistry*, *52*(0), 29-32.

806 Kaiser, K., G. Guggenberger, and L. Haumaier (2003), Organic phosphorus in soil water
807 under a European beech (Fagus sylvatica L.) stand in northeastern Bavaria, Germany:
808 seasonal variability and changes with soil depth, *Biogeochemistry*, *66*(3), 287-310.

809 Kaye, J. P., and S. C. Hart (1997), Competition for nitrogen between plants and soil
810 microorganisms, *Trends in Ecology & Evolution*, *12*(4), 139-143.

811 Kleja, D. B., M. Svensson, H. Majdi, P.-E. Jansson, O. Langvall, B. Bergkvist, M.-B.
812 Johansson, P. Weslien, L. Truusb, and A. Lindroth (2008), Pools and fluxes of carbon in
813 three Norway spruce ecosystems along a climatic gradient in Sweden, *Biogeochemistry*,
814 *89*(1), 7-25.

815 Knoll, M. A., and W. C. James (1987), Effect of the advent and diversification of vascular
816 land plants on mineral weathering through geologic time, *Geology*, *15*(12), 1099-1102.

817 Kreutzer, K., C. Beier, M. Bredemeier, K. Blanck, T. Cummins, E. Farrell, N. Lammersdorf,
818 L. Rasmussen, A. Rothe, and P. De Visser (1998), Atmospheric deposition and soil
819 acidification in five coniferous forest ecosystems: a comparison of the control plots of the
820 EXMAN sites, *Forest Ecology and Management*, *101*(1), 125-142.

821 Lamersdorf, N. P., and M. Meyer (1993), Nutrient cycling and acidification of a northwest
822 German forest site with high atmospheric nitrogen deposition, *Forest Ecology and*
823 *Management*, *62*(1–4), 323-354.

824 Leifeld, J., S. Bassin, F. Conen, I. Hajdas, M. Egli, and J. Fuhrer (2013), Control of soil pH
825 on turnover of belowground organic matter in subalpine grassland, *Biogeochemistry*, *112*(1-
826 3), 59-69.

827 Lottig, N. R., E. H. Stanley, and J. T. Maxted (2012), Assessing the influence of upstream
828 drainage lakes on fluvial organic carbon in a wetland-rich region, *Journal of Geophysical*
829 *Research: Biogeosciences (2005–2012)*, *117*(G3).

830 MacDonald, J., N. Dise, E. Matzner, M. Armbruster, P. Gundersen, and M. Forsius (2002),
831 Nitrogen input together with ecosystem nitrogen enrichment predict nitrate leaching from
832 European forests, *Global Change Biology*, *8*(10), 1028-1033.

833 Mackenzie, F. T., L. M. Ver, and A. Lerman (2002), Century-scale nitrogen and phosphorus
834 controls of the carbon cycle, *Chemical Geology*, *190*(1), 13-32.

835 Mahowald, N., et al. (2008), Global distribution of atmospheric phosphorus sources,
836 concentrations and deposition rates, and anthropogenic impacts, *Global Biogeochemical*
837 *Cycles*, *22*(4), GB4026.

838 Majer, V., B. J. Cosby, J. Kopácek, and J. Veselý (0001), Modelling reversibility of Central
839 European mountain lakes from acidification: Part I - the Bohemian forest, *Hydrol. Earth Syst.*
840 *Sci.*, *7*(4), 494-509.

841 Manzoni, S., and A. Porporato (2009), Soil carbon and nitrogen mineralization: theory and
842 models across scales, *Soil Biology and Biochemistry*, *41*(7), 1355-1379.

843 Mavris, C., M. Egli, M. Plötze, J. D. Blum, A. Mirabella, D. Giaccai, and W. Haeberli
844 (2010), Initial stages of weathering and soil formation in the Morteratsch proglacial area
845 (Upper Engadine, Switzerland), *Geoderma*, *155*(3), 359-371.

846 McCarthy, H. R., R. Oren, K. H. Johnsen, A. Gallet-Budynek, S. G. Pritchard, C. W. Cook,
847 S. L. LaDeau, R. B. Jackson, and A. C. Finzi (2010), Re-assessment of plant carbon
848 dynamics at the Duke free-air CO2 enrichment site: interactions of atmospheric [CO2] with
849 nitrogen and water availability over stand development, *New Phytologist*, *185*(2), 514-528.

850 McGill, W., and C. Cole (1981), Comparative aspects of cycling of organic C, N, S and P
851 through soil organic matter, *Geoderma*, *26*(4), 267-286.

852 McGroddy, M. E., W. T. Baisden, and L. O. Hedin (2008), Stoichiometry of hydrological C,
853 N, and P losses across climate and geology: An environmental matrix approach across New
854 Zealand primary forests, *Global Biogeochemical Cycles*, *22*(1), GB1026.

855 Mills, R., E. Tipping, C. Bryant, and B. Emmett (2014), Long-term organic carbon turnover
856 rates in natural and semi-natural topsoils, *Biogeochemistry*, *118*(1-3), 257-272.

857 Mills, R. T. E., E. Tipping, C. L. Bryant, and B. A. Emmett (2014), Long-term organic
858 carbon turnover rates in natural and semi-natural topsoils, *Biogeochemistry*, *118*(1-3), 257-
859 272.

860 Mol-Dijkstra, J., and H. Kros (1999), Modelling effects of acid deposition and climate change
861 on soil and run-off chemistry at Risdalsheia, Norway, *Hydrology and Earth System Sciences*,
862 *5*(3), 487-498.

863 Morford, S. L., B. Z. Houlton, and R. A. Dahlgren (2011), Increased forest ecosystem carbon
864 and nitrogen storage from nitrogen rich bedrock, *Nature*, *477*(7362), 78-81.

865 Moulton, K. L., and R. A. Berner (1998), Quantification of the effect of plants on weathering:
866 Studies in Iceland, *Geology*, *26*(10), 895-898.

867 Moulton, K. L., J. West, and R. A. Berner (2000), Solute flux and mineral mass balance
868 approaches to the quantification of plant effects on silicate weathering, *American Journal of*
869 *Science, 300*(7), 539-570.

870 Neal, C., B. Reynolds, M. Neal, L. Hill, H. Wickham, and B. Pugh (2003), Nitrogen in
871 rainfall, cloud water, throughfall, stemflow, stream water and groundwater for the Plynlimon
872 catchments of mid-Wales, *Sci Total Environ, 314-316*, 121-151.

873 Olander, L. P., and P. M. Vitousek (2000), Regulation of soil phosphatase and chitinase
874 activityby N and P availability, *Biogeochemistry, 49*(2), 175-191.

875 Oulehle, F., C. D. Evans, J. Hofmeister, R. Krejci, K. Tahovska, T. Persson, P. Cudlin, and J.
876 Hruska (2011), Major changes in forest carbon and nitrogen cycling caused by declining
877 sulphur deposition, *Global Change Biology, 17*(10), 3115-3129.

878 Parr, T., W. Scott, and A. Lane (1998), The UK Environmental Change Network, *The*
879 *International Long Term Ecological Research Network*, 65-73.

880 Parton, W. (1996), The CENTURY model, in *Evaluation of soil organic matter models*,
881 edited, pp. 283-291, Springer.

882 Parton, W., J. Neff, and P. M. Vitousek (2005), *Modelling phosphorus, carbon and nitrogen*
883 *dynamics in terrestrial ecosystems*, CABI.

884 Pennington, W. (1984), Long-term natural acidification of upland sites in Cumbria: evidence
885 from post-glacial lake sediments.

886 Phillips, J. D., A. V. Turkington, and D. A. Marion (2008), Weathering and vegetation effects
887 in early stages of soil formation, *Catena, 72*(1), 21-28.

888 Pilkington, M. G., S. J. Caporn, J. A. Carroll, N. Cresswell, J. A. Lee, B. Reynolds, and B. A.
889 Emmett (2005), Effects of increased deposition of atmospheric nitrogen on an upland moor:
890 nitrogen budgets and nutrient accumulation, *Environmental Pollution*, *138*(3), 473-484.

891 Qualls, R. G., and B. L. Haines (1991), Geochemistry of dissolved organic nutrients in water
892 percolating through a forest ecosystem, *Soil Science Society of America Journal*, *55*(4), 1112-
893 1123.

894 Quinn Thomas, R., C. D. Canham, K. C. Weathers, and C. L. Goodale (2010), Increased tree
895 carbon storage in response to nitrogen deposition in the US, *Nature Geosci, 3*(1), 13-17.

896 Quirk, J., D. J. Beerling, S. A. Banwart, G. Kakonyi, M. E. Romero-Gonzalez, and J. R.
897 Leake (2012), Evolution of trees and mycorrhizal fungi intensifies silicate mineral
898 weathering, *Biology letters*, *8*(6), 1006-1011.

899 Raich, J., W. Parton, A. Russell, R. Sanford, Jr., and P. Vitousek (2000), Analysis of factors
900 regulating ecosystemdevelopment on Mauna Loa using the Century model, *Biogeochemistry*,
901 *51*(2), 161-191.

902 Richardson, S., D. Peltzer, R. Allen, M. McGlone, and R. Parfitt (2004), Rapid development
903 of phosphorus limitation in temperate rainforest along the Franz Josef soil chronosequence,
904 *Oecologia*, *139*(2), 267-276.

905 Rowe, E. C., S. M. Smart, V. H. Kennedy, B. A. Emmett, and C. D. Evans (2008), Nitrogen
906 deposition increases the acquisition of phosphorus and potassium by heather Calluna
907 vulgaris, *Environmental Pollution*, *155*(2), 201-207.

Schmidt, I. K., A. Tietema, D. Williams, P. Gundersen, C. Beier, B. A. Emmett, and M. Estiarte (2004), Soil solution chemistry and element fluxes in three European heathlands and their responses to warming and drought, *Ecosystems*, *7*(6), 638-649.

Schmidt, S. K., et al. (2008), *The earliest stages of ecosystem succession in high-elevation (5000 metres above sea level), recently deglaciated soils*, 2793-2802 pp.

Schöpp, W., M. Posch, S. Mylona, and M. Johansson (2003), Long-term development of acid deposition (1880? 2030) in sensitive freshwater regions in Europe, *Hydrology and Earth System Sciences Discussions*, *7*(4), 436-446.

Schumann, U., and H. Huntrieser (2007), The global lightning-induced nitrogen oxides source, *Atmos. Chem. Phys.*, *7*(14), 3823-3907.

Shepon, A., H. Gildor, L. J. Labrador, T. Butler, L. N. Ganzeveld, and M. G. Lawrence (2007), Global reactive nitrogen deposition from lightning NOx, *Journal of Geophysical Research: Atmospheres*, *112*(D6), n/a-n/a.

Sjøeng, A. M. S., Ø. Kaste, K. Tørseth, and J. Mulder (2007), N leaching from small upland headwater catchments in southwestern Norway, *Water, Air, and Soil Pollution*, *179*(1-4), 323-340.

Speed, J. D., V. Martinsen, A. Mysterud, J. Mulder, Ø. Holand, and G. Austrheim (2014), Long-Term Increase in Aboveground Carbon Stocks Following Exclusion of Grazers and Forest Establishment in an Alpine Ecosystem, *Ecosystems*, *17*(7), 1138-1150.

Speed, J. D. M., V. Martinsen, A. J. Hester, Ø. Holand, J. Mulder, A. Mysterud, and G. Austrheim (2015), Continuous and discontinuous variation in ecosystem carbon stocks with elevation across a treeline ecotone, *Biogeosciences*, *12*(5), 1615-1627.

Sutton, M. A., A. Bleeker, C. Howard, M. Bekunda, B. Grizzetti, W. d. Vries, H. van Grinsven, Y. Abrol, T. Adhya, and G. Billen (2013), *Our Nutrient World: the challenge to produce more food and energy with less pollution*, Centre for Ecology and Hydrology (CEH).

Taylor, L., J. Leake, J. Quirk, K. Hardy, S. Banwart, and D. Beerling (2009), Biological weathering and the long-term carbon cycle: integrating mycorrhizal evolution and function into the current paradigm, *Geobiology*, *7*(2), 171-191.

Taylor, L. L., S. A. Banwart, P. J. Valdes, J. R. Leake, and D. J. Beerling (2012), Evaluating the effects of terrestrial ecosystems, climate and carbon dioxide on weathering over geological time: a global-scale process-based approach, *Philosophical Transactions of the Royal Society B: Biological Sciences*, *367*(1588), 565-582.

Tietema, A., W. De Boer, L. Riemer, and J. Verstraten (1992), Nitrate production in nitrogen-saturated acid forest soils: vertical distribution and characteristics, *Soil Biology and Biochemistry*, *24*(3), 235-240.

Tipping, E., S. Thacker, D. Wilson, and J. Hall (2008), Long-term nitrate increases in two oligotrophic lakes, due to the leaching of atmospherically-deposited N from moorland ranker soils, *Environmental Pollution*, *152*(1), 41-49.

Tipping, E., S. A. Thacker, D. Wilson, and J. R. Hall (2008), Long-term nitrate increases in two oligotrophic lakes, due to the leaching of atmospherically-deposited N from moorland ranker soils, *Environmental Pollution*, *152*(1), 41-49.

Tipping, E., P. M. Chamberlain, C. L. Bryant, and S. Buckingham (2010), Soil organic matter turnover in British deciduous woodlands, quantified with radiocarbon, *Geoderma*, *155*(1–2), 10-18.

Tipping, E., P. M. Chamberlain, M. Fröberg, P. J. Hanson, and P. M. Jardine (2012), Simulation of carbon cycling, including dissolved organic carbon transport, in forest soil locally enriched with 14C, *Biogeochemistry*, *108*(1-3), 91-107.

Tipping, E., E. Rowe, C. Evans, R. Mills, B. Emmett, J. Chaplow, and J. Hall (2012), N14C: A plant–soil nitrogen and carbon cycling model to simulate terrestrial ecosystem responses to atmospheric nitrogen deposition, *Ecological Modelling*, *247*, 11-26.

Tipping, E., et al. (2014), Atmospheric deposition of phosphorus to land and freshwater, *Environmental Science: Processes & Impacts*, *16*(7), 1608-1617.

van Meeteren, M., A. Tietema, E. Van Loon, and J. Verstraten (2008), Microbial dynamics and litter decomposition under a changed climate in a Dutch heathland, *Applied Soil Ecology*, *38*(2), 119-127.

van Veen, J., and E. Paul (1981), Organic carbon dynamics in grassland soils. 1. Background information and computer simulation, *Canadian Journal of Soil Science*, *61*(2), 185-201.

van Vuuren, D. P., A. Bouwman, and A. Beusen (2010), Phosphorus demand for the 1970–2100 period: a scenario analysis of resource depletion, *Global Environmental Change*, *20*(3), 428-439.

Ver, L. M. B., F. T. Mackenzie, and A. Lerman (1999), Biogeochemical responses of the carbon cycle to natural and human perturbations: past, present, and future, *American Journal of Science*, *299*(7-9), 762.

Vitousek, P. M., S. Porder, B. Z. Houlton, and O. A. Chadwick (2010), Terrestrial phosphorus limitation: mechanisms, implications, and nitrogen-phosphorus interactions, *Ecological Applications*, *20*(1), 5-15.

Vitousek, P. M., J. D. Aber, R. W. Howarth, G. E. Likens, P. A. Matson, D. W. Schindler, W. H. Schlesinger, and D. G. Tilman (1997), Human alteration of the global nitrogen cycle: sources and consequences, *Ecological Applications*, *7*(3), 737-750.

Volk, T. (1987), Feedbacks between weathering and atmospheric CO2 over the last 100 million years, *Am. J. Sci*, *287*(8), 763-779.

von Oheimb, G., W. Härdtle, P. S. Naumann, C. Westphal, T. Assmann, and H. Meyer (2008), Long-term effects of historical heathland farming on soil properties of forest ecosystems, *Forest Ecology and Management*, *255*(5), 1984-1993.

Walker, A. P., et al. (2015), Predicting long-term carbon sequestration in response to CO2 enrichment: How and why do current ecosystem models differ?, *Global Biogeochemical Cycles*, *29*(4), 476-495.

Walker, T., and A. F. R. Adams (1958), Studies on soil organic matter: i. Influence of phosphorus content of parent materials on accumulations of carbon, nitrogen, sulfur, and organic phosphorus in grassland soils, *Soil Science*, *85*(6), 307-318.

Walker, T., and J. K. Syers (1976), The fate of phosphorus during pedogenesis, *Geoderma*, *15*(1), 1-19.

Walse, C., B. Berg, and H. Sverdrup (1998), Review and synthesis of experimental data on organic matter decomposition with respect to the effect of temperature, moisture, and acidity, *Environmental Reviews*, *6*(1), 25-40.

993 Walthert, L., S. Zimmermann, P. Blaser, J. Luster, and P. Lüscher (2004), Waldböden der
994 Schweiz Band 1. Grundlagen und Region Jura (150-163). Birmensdorf, Eidgenössische
995 Forschungsanstalt WSL. Bern, edited, Hep Verlag.

996 Wang, Y., R. Law, and B. Pak (2010), A global model of carbon, nitrogen and phosphorus
997 cycles for the terrestrial biosphere, *Biogeosciences*, *7*(7), 2261-2282.

998 Weng, L., F. Vega, and W. Van Riemsdijk (2011), Competitive and synergistic effects in pH
999 dependent phosphate adsorption in soils: LCD modeling, *Environmental science &*
1000 *technology*, *45*(19), 8420.

1001 White, A. F., A. E. Blum, T. D. Bullen, D. V. Vivit, M. Schulz, and J. Fitzpatrick (1999), The
1002 effect of temperature on experimental and natural chemical weathering rates of granitoid
1003 rocks, *Geochimica et Cosmochimica Acta*, *63*(19), 3277-3291.

1004 Wright, R., C. Beier, and B. Cosby (1998), Effects of nitrogen deposition and climate change
1005 on nitrogen runoff at Norwegian boreal forest catchments: the MERLIN model applied to
1006 Risdalsheia (RAIN and CLIMEX projects), *Hydrology and Earth System Sciences*
1007 *Discussions*, *2*(4), 399-414.

1008 Yanai, R. (1992), Phosphorus budget of a 70-year-old northern hardwood forest,
1009 *Biogeochemistry*, *17*(1), 1-22.

1010 Yang, X., W. M. Post, P. E. Thornton, and A. Jain (2013), The distribution of soil phosphorus
1011 for global biogeochemical modeling, *Biogeosciences*, *10*(4), 2525-2537.

1012 Yang, X., P. Thornton, D. Ricciuto, and W. Post (2014), The role of phosphorus dynamics in
1013 tropical forests–a modeling study using CLM-CNP, *Biogeosciences*, *11*(6), 1667-1681.

1014 Zimmermann, S., and S. u. L. E. F. f. Wald (2006), *Waldböden der Schweiz. 3. Regionen*
1015 *Mittelland und Voralpen*, hep-Verlag.

1016

1017

Tables

Table 1: Model state variable and output variable notation

Variables	Description	Units
	State variables	
$C, N, P_{bio,fine/coarse}$	C, N and P stored in fine and coarse plant tissues	g m^{-2}
C, N, P_{lit}	C, N and P stored in coarse litter	g m^{-2}
$C, N, P_{SOM,i}$	C, N and P stored in compartment i (fast/slow/passive) of the SOM	g m^{-2}
P_{sorb}	Inorganic phosphorus sorbed to soil surfaces	g m^{-2}
P_{weath}	Weatherable phosphorus within accessible substrate	g m^{-2}
BC_{weath}	Weatherable BCs within accessible substrate	g m^{-2}
$P_{fixavail}$	P available for fixation	g m^{-2}
N,$P_{\text{avail,excess}}$	N and P available for plant growth, and excess after growth	g m^{-2}
	Output variables	
$\Delta C, N, P_{DO}$	Output of dissolved organic C, N and P from SOM	g m^{-2} dt^{-1}
$\Delta N, P_{inorg}$	Output of dissolved inorganic N and P from SOM	g m^{-2} dt^{-1}
$\Delta P_{sorbed/desorbed}$	Inorganic P sorbed/desorbed from soil surfaces	g m^{-2} dt^{-1}
ΔN_{fix}	N fixation in topsoil	g m^{-2} dt^{-1}
$\Delta N, P_{retained}$	N, P remobilized from foiliage before litterfall	g m^{-2} dt^{1}
$\Delta N, P_{demand,i}$	N, P demand for plant growth for plant species end member i	g m^{-2} dt^{-1}
NPP_{pot}, NPP_{act}	Potential and actual net primary productivity	gC m^{-2} dt^{-1}
$\Delta P, BC_{weath}$	Phosphorus and base cation weathering flux	g m^{-2} dt^{-1}
$\Delta N, P_{immob}$	Immobilization flux of N and P	g m^{-2} dt^{-1}
	Input variables	
$\Delta N, P, BC_{dep}$	Deposition of N, P and BCs	g m^{-2} dt^{-1}
T	Mean quarterly temperature	°C
$F_{T>0}$	Fraction of year with temperatures below zero	-

1021 Table 2: Parameter notation used in main text

Notation	Description	Units
f_{DO}	fractional release of DOC, DON and DOP in decomposition	proportion
$f_{dep,bypass}$	fraction of deposition bypassing the topsoil	proportion
k_{immobN}	rate constant for N uptake by SOM	dt^{-1}
β_{immobP}	proportionality constant between P immobilization rate constant and N immobilization rate constant(s).	-
$[C:N]_{im,lower}$	C:N lower limit on immobilization of N into SOM	$g\ g^{-1}$
$[C:N]_{im,upper}$	C:N upper limit on immobilization of N into SOM	$g\ g^{-1}$
$[C:P]_{im,lower}$	C:P lower limit on immobilization of P into SOM	$g\ g^{-1}$
$[C:P]_{im,upper}$	C:P upper limit on immobilization of P into SOM	$g\ g^{-1}$
k_{sorb}	rate constant for sorption of dissolved inorganic P to soil surfaces	dt^{-1}
k_{desorb}	rate constant for desorption of inorganic P from soil surfaces	dt^{-1}
k_{Nfix}	parameter relating N fixation to P availability	$gN\ gP^{-1}\ m^{-2}$
N_{fixmax}	maximum N fixation	$g\ m^{-2}\ dt^{-1}$
$[C:P]_{fixlim}$	C:P ratio limit on P extraction from SOM by root exudates	$g\ g^{-1}$
Q_{10}	change in rate with 10 ^{o}C increase in temperature	-
$K_{acid,}\ n_{acid}$	parameters describing relation of immob. and decomp. to pH	
$k_{Pweath,}$ $k_{BCweath}$	Weathering rates for phosphorus and base cation pools	dt^{-1}
P_{weath0}	Initial weatherable phosphorus within accessible substrate	$g\ m^{-2}$
BC_{weath0}	Initial weatherable BCs within accessible substrate	$g\ m^{-2}$

1022

1023

Table 3: Model parameter values set within the generalized parameterization. The second column from the left gives the range of parameter values found from a set of 50 localized searches and the search boundaries (in square brackets). Following these searches the first four parameters were found to be well constrained and set as shown in the third column from the left. A globalized search was then performed on the remaining 4 parameters, resulting in parameter values as shown in the last column.

Parameter	Range from 50 local searches [boundaries]	Parameter set through multiple local searches	Parameter set by reduced global search
f_{DO}	0.03-0.032 [0.001, 0.1]	0.0308	-
P_{weath0}	100-149 [100, 1000]	120	-
k_{Nfix}	0.025-0.040 [0.02, 0.2]	0.0286	-
f_{Psorb}	0.94-0.99 [0.8, 0.99]	0.97	-
$k_{immobP:N}$	4.29-19.88 [0.1, 10]	-	8.58
$f_{Pdesorb}$	0.005-0.049 [0.01, 0.05]	-	0.005
K_{acid}	0.024-0.485[1e-6, 0.5]	-	0.364
n_{acid}	0.38-1 [0.1, 1]	-	0.590

Figure captions

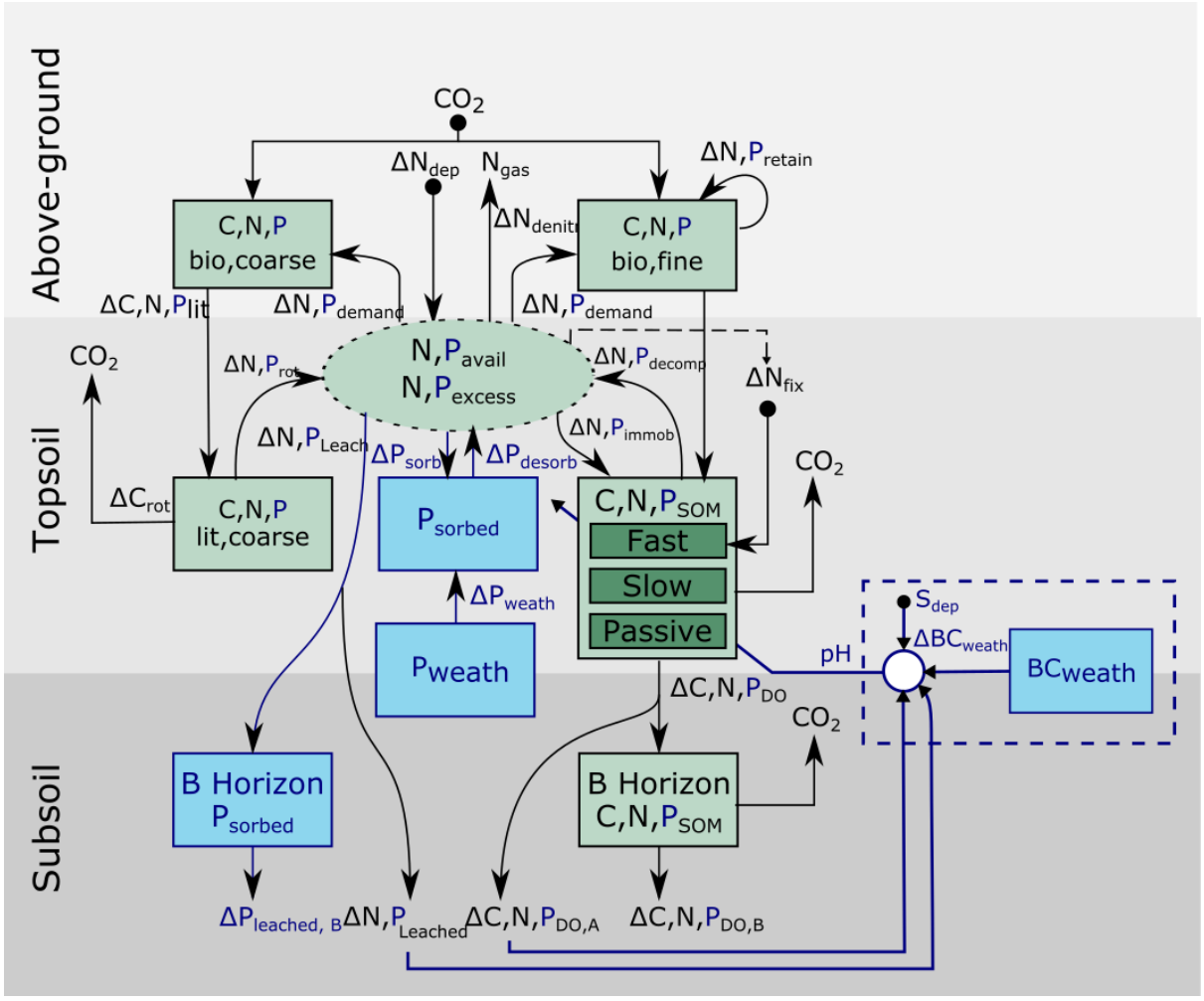

Figure 1: Overview of carbon nitrogen and phosphorus stocks and flows simulated in the N14CP model. New additions in N14CP compared with N14C are highlighted in blue.

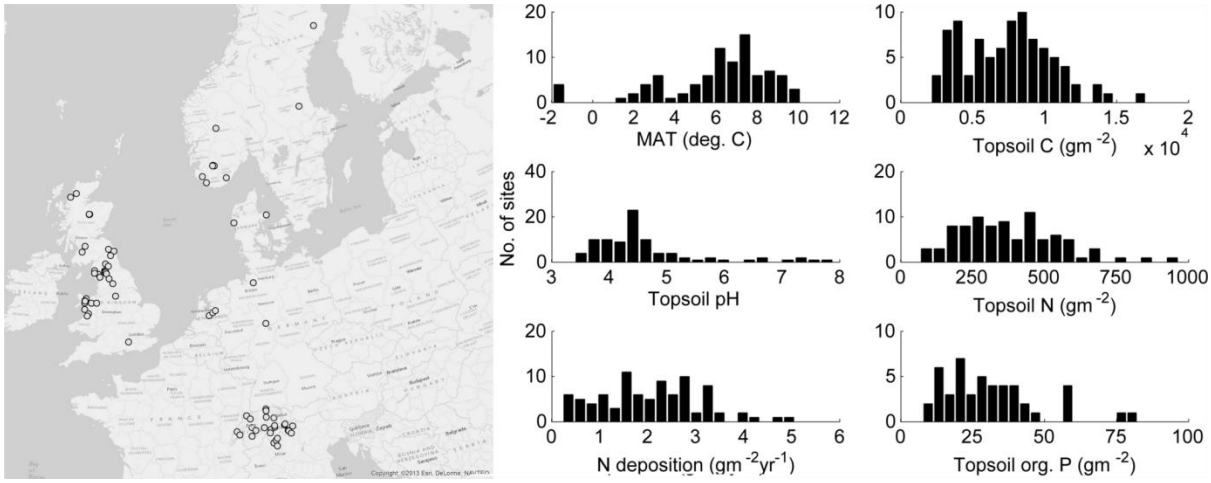

Figure 2: Site data locations and distributions of Mean Annual Temperature (MAT), soil pH, nitrogen deposition in year 2000, and observed organic topsoil carbon, nitrogen and phosphorus contents. Data is detailed in the SI, Tables S3-5 [*Andersson et al.*, 2002; *Beier et al.*, 2009; *Berggren et al.*, 2004; *Blaser et al.*, 2005; *Bloemerts and Vries*, 2009; *Corre and Lamersdorf*, 2004; *de Vries et al.*, 2005; *DEFRA*; *defra*; *B A Emmett et al.*, 2004; *Evans et al.*, 2005; *Gundersen*, 1995; *Jackson-Blake et al.*, 2012; *Kleja et al.*, 2008; *Kreutzer et al.*, 1998; *Lamersdorf and Meyer*, 1993; *MacDonald et al.*, 2002; *Mol-Dijkstra and Kros*, 1999; *Parr et al.*, 1998; *Pilkington et al.*, 2005; *I K Schmidt et al.*, 2004; *Sjøeng et al.*, 2007; *J D Speed et al.*, 2014; *J D M Speed et al.*, 2015; *Tietema et al.*, 1992; *E Tipping et al.*, 2008; *van Meeteren et al.*, 2008; *von Oheimb et al.*, 2008; *Walthert et al.*, 2004; *Wright et al.*, 1998; *Zimmermann and Wald*, 2006].

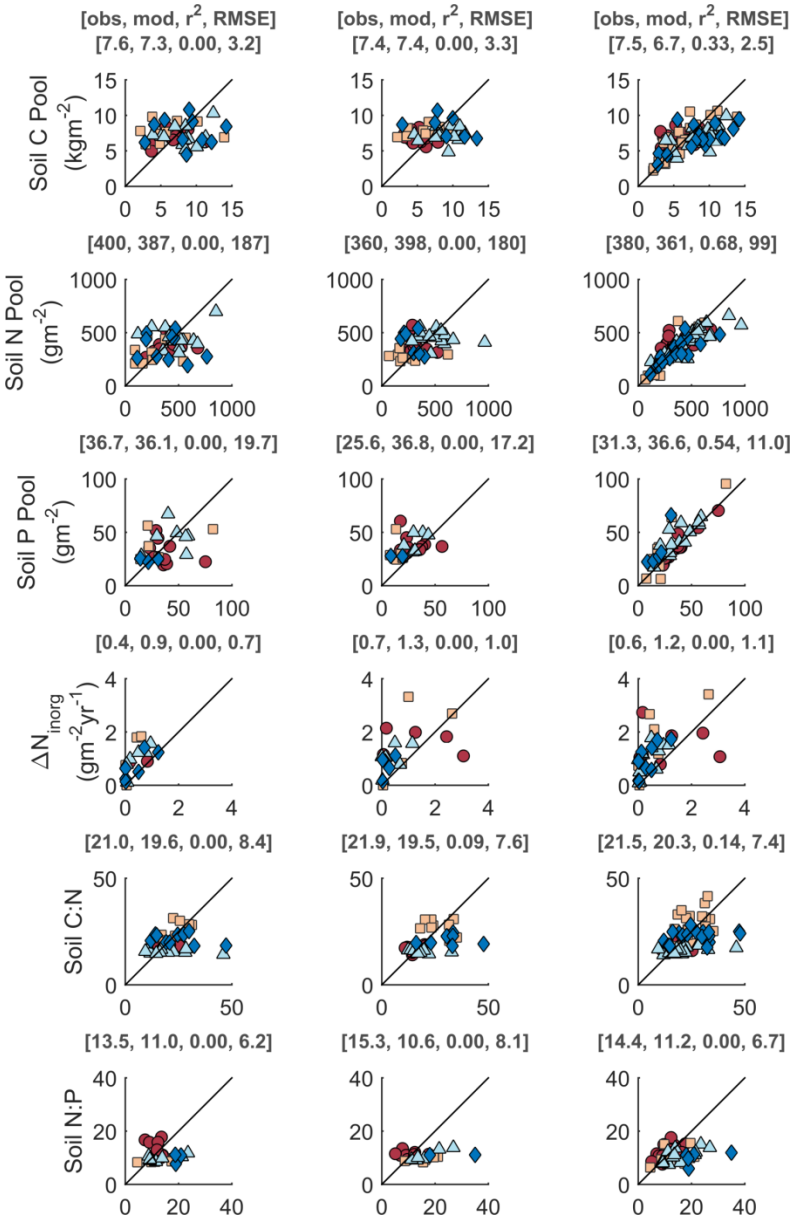

Figure 3: Observations (x axis) vs. N14CP model simulations (y axis). Left column: Observations and model outputs for parameterization sites using the generalized parameter set. Middle column: Observations and model outputs for test sites using the generalized parameter set. Right column: Observations and model outputs for all sites in the dataset when the initial pool of weatherable P is allowed to vary on a site by site basis and the value of Pweath0 is chosen by minimizing the site observation-mode residuals. Contemporary plant cover is denoted by marker style: broadleaf forest is denoted by a circle, coniferous forest by a square, shrubland by a diamond, and herbaceous plant cover by a triangle. Lines are the one-to-one relationship between observation and model. The mean of the observations and the model, and the r^2 and root mean square errors (RMSE) are given in the titles.

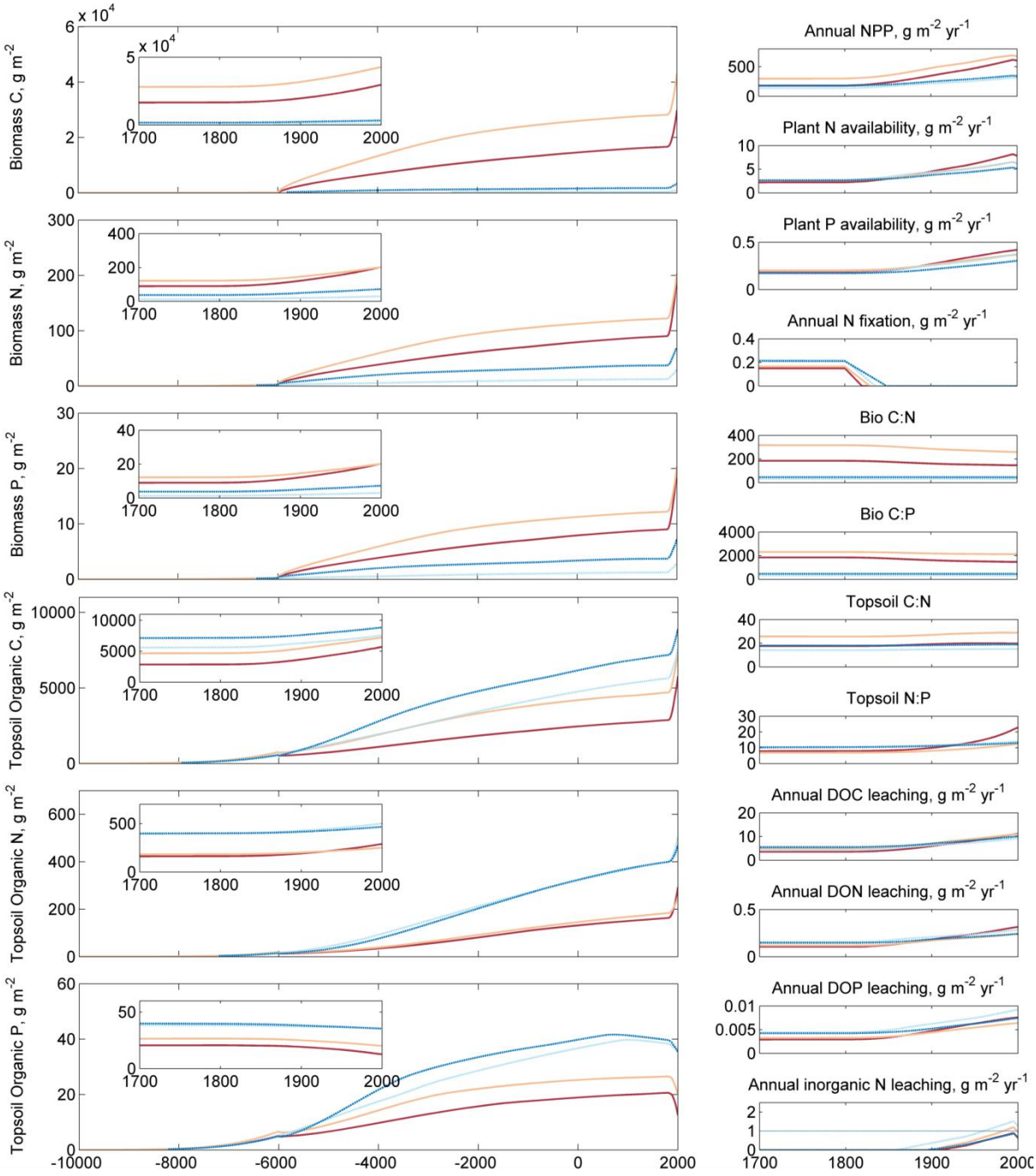

Figure 4: Time-series results using the generalized parameter set for four sites with varying plant functional type (broadleaf: red line, conifer: yellow line, herbaceous: light blue, shrub: dark blue line), driven with median climate and deposition conditions. All sites start with herbaceous vegetation and transition to their modern day vegetation type in 6000BC (broadly concurring with estimates of northern Europe succession dates post-glaciation).

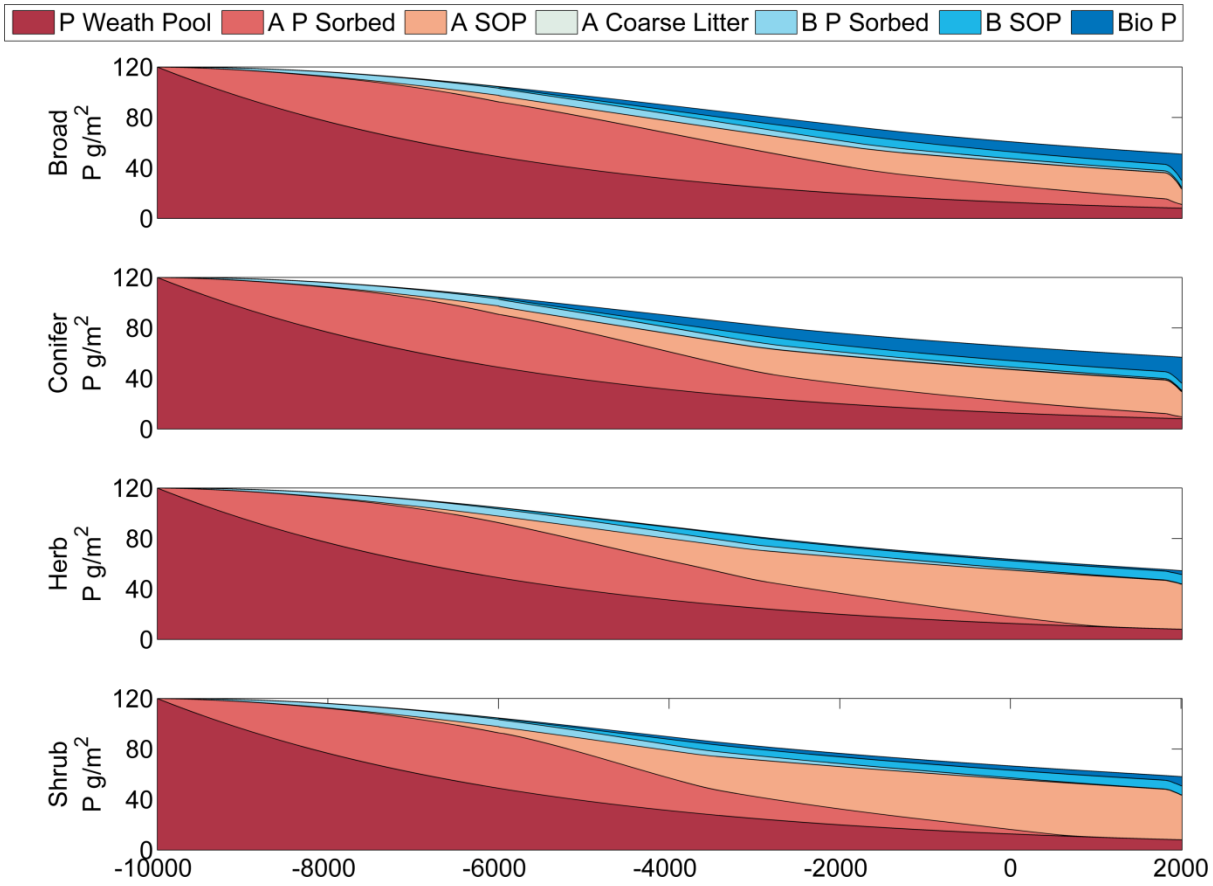

Figure 5: Changes in modelled P stores between 10000 BC, which marks the recession of the ice and commencement of weathering, to 2000 AD. As for Figure 4, the model was driven with median climate and deposition conditions.

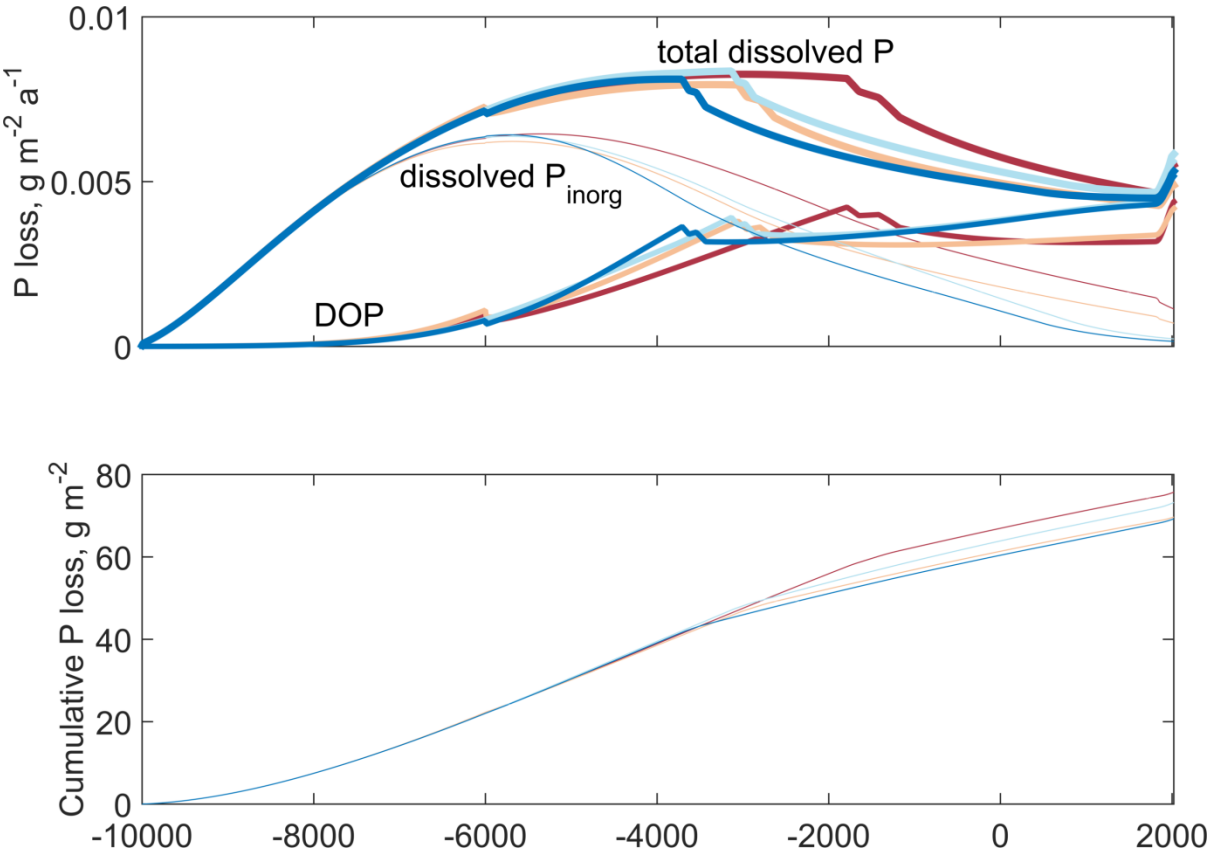

Figure 6: Leaching losses of P, modelled with median climate and deposition conditions. Top panel: inorganic, organic and total fluxes for different PFT (broadleaf: red line, conifer: yellow line, herbaceous: light blue, shrub: dark blue line). Lower panel: cumulative losses.